

# Computing feasible trajectories for constrained maneuvering systems: the PVTOL example<sup>★</sup>

Giuseppe Notarstefano<sup>a</sup> and John Hauser<sup>b</sup>

<sup>a</sup>*Department of Engineering, University of Lecce, Via per Monteroni, 73100 Lecce, Italy*

`giuseppe.notarstefano@unile.it`

<sup>b</sup>*Department of Electrical and Computer Engineering, University of Colorado, Boulder, CO 80309-0425, USA*

`hauser@colorado.edu`

---

## Abstract

In this paper we provide an optimal control based strategy to explore *feasible trajectories* of nonlinear systems, that is to find curves that satisfy the dynamics as well as point-wise state-input constraints. The strategy is interesting itself in understanding the capabilities of the system in its operating region, and represents a preliminary tool to perform trajectory tracking in presence of constraints. The strategy relies on three main tools: dynamic embedding, constraints relaxation and novel optimization techniques, introduced in [10,12], to find regularized solutions for *point-wise* constrained optimal control problems. The strategy is applied to the PVTOL, a simplified model of a real aircraft that captures the main features and challenges of several “maneuvering systems”.

*Key words:* Nonlinear optimal control, constrained optimization, VTOL aircraft, nonlinear inversion.

---

## 1 Introduction

In several fields as aerospace, robotics and automotive, designers have to deal with complex nonlinear system dynamics. A deep knowledge of the behavior of such systems is fundamental both in controlling them about a (possibly aggressive) desired trajectory and in assisting the engineer in the design process. An interesting problem is, therefore, the exploration of the trajectory manifold of the system, that is, the characterization of the system (state-input) trajectories and their parametrization with respect to “performance-output curves”. More formally, given a desired curve for some of the states (outputs), we aim at finding a state-input *lifted trajectory* (i.e. a state-input curve satisfying the dynamics) whose outputs are close to the desired ones. The solution of this problem is interesting itself in understanding the behavior of the system and provides a nominal trajectory that can be used in a receding horizon scheme for trajectory tracking.

Having in mind engineering applications, there is an important aspect to take into account in the solution of exploration and tracking, that is the presence of constraints in the system. Such constraints may arise from diverse causes such as: physical bounds on the states and the inputs, validity bounds of the model or presence (respectively absence) of important properties (e.g. controllability). We will call the region where constraints are satisfied *feasibility region*. This implies that, not only we look for lifted trajectories (curves satisfying the dynamics), but furthermore we ask for *feasible lifted trajectories*, that is trajectories lying in the feasibility region.

In this paper we concentrate our attention on a special class of nonlinear systems that we call *maneuvering systems*. In this class we include those systems for which a natural notion of performance outputs is present. Namely, some

---

<sup>★</sup> This paper was not presented at any IFAC meeting. Preliminary versions of this work with partial results were presented as [26,25]. Corresponding author G. Notarstefano, `giuseppe.notarstefano@unile.it`. Tel. +390832297360 Fax +39 0832 297733.

of the states are requested to follow (almost exactly) a desired profile, while the remaining states meet suitable (feasibility) bounds. Maneuvering systems include for example vehicles (cars, motorcycles, aerial vehicles, marine vehicles), manipulators and several other mechanical systems. In this paper we consider as “prototype example” of maneuvering system the PVTOL aircraft. The PVTOL was introduced by Hauser et al. in [15] in order to capture the lateral non-minimum phase behavior of a Vertical Take Off and Landing (VTOL) aircraft. This model has been widely studied in the literature for its property of combining important features of nonlinear systems with “tractable” equations. Furthermore, the dynamics of many other mechanical (maneuvering) systems can be rewritten in a similar fashion, e.g., the cart-pole system, the pendubot [30], the bicycle model [9], [13] and the longitudinal dynamics of a real aircraft. Since the PVTOL has been introduced in 1992, many researchers have studied this system. A non exhaustive literature review of works on trajectory tracking or path following of the PVTOL includes [15,29,1,21,5,4].

The trajectory exploration problem has been investigated in the literature in different formulations. Trajectory exploration for a class of VTOL aircrafts is tackled in [24], where an optimization strategy is proposed to compute optimal transition maneuvers. The problem of finding a (state-input) trajectory whose output is exactly an assigned desired curve is known in the literature as nonlinear inversion. This problem is particularly challenging for nonminimum-phase systems. The problem was introduced and solved for some classes of nonlinear systems and desired output curves in [7] and extended to time-varying and non-hyperbolic systems respectively in [8] and [6]. More recently, [28], a new approach based on the notion of convergent systems was proposed to solve the problem. In [14] the nonlinear inversion problem was solved for an inverted pendulum by use of exponential dichotomy under mild conditions on the output curve. Nonlinear inversion is strongly related to the output regulation problem, that is to the design of a control law such that the system output asymptotically tracks a desired output curve. An early reference is [19]. There, the nonlinear inversion problem was solved by means of a suitable partial differential equation when the desired output curve is the trajectory of an exosystem. In [17] a two-step strategy was proposed to solve the stable inversion problem. An overview on the topic can be found in [3], whereas more recent references include [20,16,27].

The contribution of the paper is threefold. First, we propose an optimal control based strategy to compute feasible trajectories of maneuvering systems. The strategy relies on three main ideas: dynamic embedding, constraints relaxation and continuation with respect to (the embedding and relaxation) parameters. In detail, we compute feasible trajectories (i.e., trajectories satisfying pointwise state and input constraints) that minimize a weighted  $L_2$  distance from the desired output curve. In order to compute an approximate solution to this problem we perform the following steps. We embed the system into a family of systems and relax the feasibility region so that the constraints are not active. For each value of the system (embedding) and constraint (relaxation) parameters, we compute an unconstrained lifted (state-input) trajectory (by applying an optimal control based dynamic embedding technique) and use it as desired curve for a constrained  $L_2$  distance minimization. To compute a feasible trajectory ( $L_2$  close to the unconstrained one), we design a relaxed version of the constrained optimal control problem. The relaxation is based on the introduction of a parametrized barrier functional to handle the constraints [12]. The resulting optimal control problem is solved by means of a projection operator based Newton method [10]. The final ingredient of the strategy is a continuation procedure to update the embedding and relaxation parameters up to their nominal values.

Second, we prove the effectiveness of the strategy, namely that a feasible lifted trajectory can be computed, for suitable values of the embedding and relaxation parameters. The proof of this result relies on the continuity and differentiability of an optimal control minimizer with respect to parameters, which is provided as a stand alone result. An analogous result was already proven in [22] for unconstrained systems and extended to input-state constrained systems in [23]. The main differences with the existing results are the following. We do not consider input and state constraints directly, but take them into account in a relaxed version of the constrained optimal control problem by use of a barrier functional, the barrier functional being weighted by one of the varying parameters. Furthermore, we take into account the system dynamics by means of a trajectory tracking projection operator. The projection operator is the key distinctive feature for the proof of the differentiability result. Indeed, the projection operator allows to convert the dynamically constrained optimal control problem into an unconstrained trajectory optimization problem. Thus, an appropriate implicit function theorem can be used to *solve* the first order necessary condition equation. The implicit function theorem allows to show that, if the second derivative of the cost composed with the projection operator is invertible at the nominal parameter, then there is a neighborhood on which the local minimizer exists and is  $\mathcal{C}^1$  with respect to the parameter. It turns out that the appropriate condition to ensure invertibility of the operator is that the minimizer satisfies the second order sufficiency condition at the nominal parameter.

Third and final, we provide a complete characterization of the exploration strategy for the PVTOL. In detail, we first solve the nonlinear inversion problem for the unconstrained PVTOL. Given any  $\mathcal{C}^4$  desired output curve resulting into a bounded acceleration profile, we prove that a trajectory can be computed for the decoupled system and for suitable positive values of the coupling parameter. Based on this result and on the second set of contributions,

we show that all the strategy steps can be performed for suitable values of the feasibility region and the coupling parameter. Finally, we perform a numerical analysis showing that, in fact, feasible trajectories of the PVTOL can be computed for aggressive desired output curves even in presence of relatively tight constraints.

The paper is organized as follows. In Section 2 the notion of maneuvering systems is introduced and the PVTOL aircraft is presented as a prototype example. Section 3 defines the performance tasks solved in the paper, namely unconstrained and constrained trajectory lifting. In Section 4 the unconstrained lifting task is solved for the PVTOL aircraft. That is, a lifted trajectory is proven to exist for some positive values of the coupling parameter. In Section 5 the proposed optimal control based exploration strategy is presented and in Section 6 a theoretical analysis of the strategy is developed, proving that for suitable values of the system and constraint parameters a feasible trajectory exists. In Section 7 numerical computations are provided showing the effectiveness of the strategy for the constrained PVTOL on an aggressive barrel roll trajectory in presence of respectively input and state-input constraints. Finally, in Appendix A an overview of the trajectory tracking projection operator theory and the projection operator based Newton method for unconstrained and constrained optimal control problems is given.

**Notation** For a function  $g : [0, T] \rightarrow \mathbb{R}^p$ ,  $T > 0$ , we let  $\|g(\cdot)\|_{L_\infty} = \sup_{t \in [0, T]} \|g(t)\|$  be the usual  $L_\infty$  norm. Let  $\mathcal{C}^k[0, T]^p$ ,  $L_\infty[0, T]^p$  and  $L_2[0, T]^p$  be the spaces of functions  $g : [0, T] \rightarrow \mathbb{R}^p$  that are respectively  $k$  times differentiable with continuous  $k$ -th derivative, bounded and Lebesgue integrable, and square integrable on  $[0, T]$ . In the rest of the paper we will abuse notation and denote them as  $\mathcal{C}^k$ ,  $L_\infty$  and  $L_2$  when domain and codomain are clear. Let  $\xi \mapsto A(\xi)$  be a twice Fréchet differentiable operator, we denote respectively  $\zeta \mapsto DA(\xi_0) \cdot \zeta$  and  $(\zeta, \eta) \mapsto D^2A(\xi_0) \cdot (\zeta, \eta)$  the first and second Fréchet differentials of  $A$  at  $\xi_0$ . Given a control system  $\dot{x} = f(x, u)$ , where  $x \in \mathbb{R}^n$  is the state and  $u \in \mathbb{R}^m$  is the control input, we say that a *bounded* curve  $\eta = (\bar{x}(\cdot), \bar{u}(\cdot))$  is a (state-control) *trajectory* of the system if  $\dot{\bar{x}}(t) = f(\bar{x}(t), \bar{u}(t))$  for all  $t \in [0, T]$ ,  $0 < T \leq +\infty$ , and  $x(0) = \bar{x}(0)$ . Trajectories of the system through  $x_0$  belong to the affine subspace  $\tilde{X} := (x_0, 0) + X_\infty$ , where  $X_\infty$  is the closed subspace of  $L_\infty^{n+m}[0, T]$  of curves  $\zeta = (\beta, \nu)$  with continuous  $\beta$ ,  $\beta(0) = 0$ , and bounded  $\nu$ . We denote  $\mathcal{T} \subset \tilde{X}$  the set of bounded (in  $L_\infty$ ) trajectories through  $x_0$ .

## 2 The PVTOL model and maneuvering system definition

In this section we introduce the system that motivates our work, the PVTOL, and inspired by this model we introduce the notion of maneuvering systems. The PVTOL aircraft was introduced in [15]. Using standard aeronautic conventions the equations of motion are given by

$$\begin{aligned} \ddot{y} &= u_1 \sin \varphi - \epsilon_P u_2 \cos \varphi \\ \ddot{z} &= -u_1 \cos \varphi - \epsilon_P u_2 \sin \varphi + g \\ \ddot{\varphi} &= u_2. \end{aligned} \tag{1}$$

The aircraft state is given by the position  $(y, z)$  of the center of gravity, the roll angle  $\varphi$  and the respective velocities  $\dot{y}$ ,  $\dot{z}$  and  $\dot{\varphi}$ . The control inputs  $u_1$  and  $u_2$  are respectively the vertical thrust force and the rolling moment. The gravity acceleration is denoted by  $g$ . An interesting feature of the PVTOL model is that the rolling moment  $u_2$  generates also a lateral force  $\epsilon_P u_2$ , where  $\epsilon_P \in \mathbb{R}$  is a coupling coefficient. In Figure 1 the PVTOL aircraft with the reference system and the inputs is shown. Depending on the value of  $\epsilon_P$  the PVTOL shows very diverse dynamic

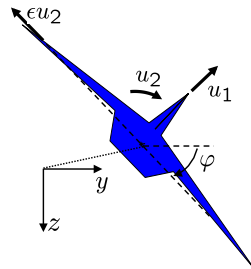


Fig. 1. PVTOL aircraft.

behaviors and possesses different control properties. We will clarify them in the next sections.

Next, we exploit an important feature of the PVTOL that can be generalized to a wide class of systems that we will refer to as *maneuvering systems*. In analyzing the PVTOL, we can partition the state space into the cartesian product of: i) *external position states* ( $y$  and  $z$ ), ii) *internal position states* ( $\varphi$ ) and iii) *velocities* ( $\dot{y}$ ,  $\dot{z}$  and  $\dot{\varphi}$ ). In many engineering applications the objective is to track a time parametrized curve described by the external position states while maintaining the internal position states bounded (the trajectories of the velocities being consistent with the related positions). Thus, a natural choice of outputs arises for these systems, namely the external position states. We call these outputs *performance outputs* meaning that a task for the system may be defined by assigning a desired curve for these states (desired performance outputs)<sup>1</sup>. From now on, since we will be only dealing with performance outputs, we will refer to them as outputs. A state space model of a maneuvering system is given by

$$\begin{aligned}\dot{x}(t) &= f(x(t), u(t)), \\ \mathbf{y}(t) &= p(x(t)), \quad t \in [0, T], \quad T > 0,\end{aligned}$$

where  $x$ ,  $u$  and  $\mathbf{y}$  are respectively the state, the input and the performance output,  $f : \mathbb{R}^n \times \mathbb{R}^m \rightarrow \mathbb{R}^n$  is assumed to be  $\mathcal{C}^2$  in both arguments, and  $p$  selects a subset of the states (e.g. the external position states for the PVTOL).

For the PVTOL, a state space model can be obtained by posing  $x = (y, z, \varphi, \dot{y}, \dot{z}, \dot{\varphi})$  and  $u = (u_1, u_2)$ . Also, a natural choice of performance outputs is given by the position of the center of gravity  $(y, z)$ , so that  $p(x) := (y, z) = (x_1, x_2)$ .

### 3 Development of performance tasks

In this section we identify important challenges that arise in studying the PVTOL capabilities and that can be generalized to maneuvering systems. These challenges will drive us in providing useful strategies to explore the dynamic capabilities of maneuvering systems.

We start defining the first two tasks we are interested in. Informally, given a time-parametrized desired output curve, we want to find a (state-control) trajectory of the system, such that the output portion of the trajectory is close to the desired output curve. We will call this task *trajectory lifting*. We will also define an approximate version of such task, called *practical trajectory lifting*, suitable for computations. More formally we can define the two tasks as follows. Given an output curve  $\alpha(\cdot) \in L_\infty[0, T]^p$ , we denote  $\|\alpha(\cdot)\|_{L_2}$  a suitable weighted  $L_2$  norm of  $\alpha(\cdot)$ , that is,  $\|\alpha(\cdot)\|_{L_2} = \int_0^T \alpha(t)^T W \alpha(t) dt + \alpha(T)^T W_1 \alpha(T)$ , with  $W$  and  $W_1$  positive definite matrices.<sup>2</sup>

**Definition 3.1 (Trajectory lifting task)** Let  $\mathbf{y}_d(t)$ ,  $t \in [0, T]$ , be a desired sufficiently smooth output curve. Find a bounded trajectory  $(x^*(\cdot), u^*(\cdot)) \in \mathcal{T}$  such that

$$\|p(x^*(\cdot)) - \mathbf{y}_d(\cdot)\|_{L_2}^2 \leq \|p(x(\cdot)) - \mathbf{y}_d(\cdot)\|_{L_2}^2 \quad \text{for all } (x(\cdot), u(\cdot)) \in \mathcal{T}$$

**Definition 3.2 (Practical trajectory lifting task)** Let  $\mathbf{y}_d(t)$ ,  $t \in [0, T]$ , be a desired sufficiently smooth output curve. For a given  $\epsilon > 0$ , find a trajectory  $(x_\epsilon^*(\cdot), u_\epsilon^*(\cdot)) \in \mathcal{T}$  such that

$$\|p(x_\epsilon^*(\cdot)) - \mathbf{y}_d(\cdot)\|_{L_2}^2 \leq \|p(x(\cdot)) - \mathbf{y}_d(\cdot)\|_{L_2}^2 + \epsilon \quad \text{for all } (x(\cdot), u(\cdot)) \in \mathcal{T}$$

**Remark 3.3 (Trajectory lifting and dynamic inversion)** *Dynamic inversion*, [7], is a trajectory lifting problem in the case the time horizon is  $(-\infty, +\infty)$ . The objective is to find a (state-input) trajectory such that the output trajectory is exactly the desired one. Clearly, if a solution to dynamic inversion exists, it is also a solution for the trajectory lifting task on the time horizon  $[0, T]$  with zero minimum cost. If such a trajectory exists we say that it exactly solves the trajectory lifting task. In the next section we will show that for the PVTOL it is in fact possible to solve the dynamic inversion problem. This could be not the case for other maneuvering systems, but (practical) trajectory lifting could still be solved by using optimal control.

**Remark 3.4 (Trajectory lifting for flat systems)** In most cases the performance outputs are driven by the application and cannot be decided by the designer. Thus, even for systems that are feedback linearizable or differentially

<sup>1</sup> The performance outputs are different from measured outputs, i.e., states or functions of states that can be measured by a sensor. Measured outputs play an important role in control design, but will not be considered here.

<sup>2</sup> If  $W = I_n$  and  $W_1 = 0$  this is the classical  $L_2$  norm.

flat, the design of a lifted trajectory is an issue. Regarding the PVTOL, in [15] it was shown that the decoupled PVTOL ( $\epsilon_P = 0$ ) was feedback linearizable, hence differentially flat, relative to the natural outputs. In [29] it was shown that the coupled PVTOL is also differentially flat, but with respect to the flat outputs  $y_f = y + \epsilon_P \sin \varphi$  and  $z_f = z + \epsilon_P \cos \varphi$ . If the flat outputs were chosen as performance outputs, the problem of finding a trajectory of the system consistent with the outputs would be easily solved as for the decoupled model. However, physical considerations suggest that the natural outputs are better suited as performance outputs.

In this paper we are interested in a more challenging task, namely a constrained version of the lifting task. That is, we want to perform the lifting task while enforcing point-wise constraints on control inputs and states. In other words, given a desired output curve and a region of the state-input space, we want to find a trajectory that lies entirely in the region and whose output portion is close (according to a given cost function) to the desired curve.

More formally, we define a *feasibility region*  $\overline{\mathcal{XU}} \subset \mathbb{R}^n \times \mathbb{R}^m$  as a compact simply connected region of the state-input space where the trajectories of the system must lie at every time. Consistently, a *feasible trajectory* for  $\overline{\mathcal{XU}}$  is a trajectory of the system,  $(x(\cdot), u(\cdot)) \in \mathcal{T}$ , such that  $(x(t), u(t)) \in \overline{\mathcal{XU}}$  for almost all  $t \in [0, T]$ . In the rest of the paper we will focus on trajectories that belong to the interior,  $\mathcal{XU}$ , of  $\overline{\mathcal{XU}}$ . Thus, we say that a trajectory of the system,  $(x(\cdot), u(\cdot)) \in \mathcal{T}$ , is a *strictly feasible trajectory* for  $\overline{\mathcal{XU}}$  if  $(x(t), u(t)) \in \mathcal{XU}$  for almost all  $t \in [0, T]$ . We are now ready to define the constrained version of the lifting task. As for the unconstrained problem we define an exact and a practical task.

**Definition 3.5 (Feasible trajectory lifting task)** Let  $\mathbf{y}_d(t)$ ,  $t \in [0, T]$ , be a desired sufficiently smooth output curve and  $\overline{\mathcal{XU}} \subset \mathbb{R}^n \times \mathbb{R}^m$  a feasibility region. Find a feasible trajectory,  $(x^*(\cdot), u^*(\cdot)) \in \mathcal{T}$  with  $(x_\epsilon^*(t), u_\epsilon^*(t)) \in \overline{\mathcal{XU}}$  for almost all  $t \in [0, T]$ , such that

$$\|p(x^*(\cdot)) - \mathbf{y}_d(\cdot)\|_{L_2}^2 \leq \|p(x(\cdot)) - \mathbf{y}_d(\cdot)\|_{L_2}^2$$

for all  $(x(\cdot), u(\cdot)) \in \mathcal{T}$  with  $(x(t), u(t)) \in \overline{\mathcal{XU}}$  for almost all  $t \in [0, T]$ .

**Definition 3.6 (Practical feasible trajectory lifting task)** Let  $\mathbf{y}_d(t)$ ,  $t \in [0, T]$ , be a desired sufficiently smooth output curve and  $\overline{\mathcal{XU}} \subset \mathbb{R}^n \times \mathbb{R}^m$  a feasibility region. For a given  $\epsilon > 0$ , find a feasible trajectory,  $(x_\epsilon^*(\cdot), u_\epsilon^*(\cdot)) \in \mathcal{T}$  with  $(x_\epsilon^*(t), u_\epsilon^*(t)) \in \overline{\mathcal{XU}}$  for almost all  $t \in [0, T]$ , such that

$$\|p(x_\epsilon^*(\cdot)) - \mathbf{y}_d(\cdot)\|_{L_2}^2 \leq \|p(x(\cdot)) - \mathbf{y}_d(\cdot)\|_{L_2}^2 + \epsilon \quad (2)$$

for all  $(x(\cdot), u(\cdot)) \in \mathcal{T}$  with  $(x(t), u(t)) \in \overline{\mathcal{XU}}$  for almost all  $t \in [0, T]$ .

Finding a global solution to the above problems is a hard task since we are dealing with infinite dimensional optimization problems. Thus, our goal in this paper is to find a feasible trajectory that satisfies locally equation (2).

## 4 Trajectory lifting for the unconstrained PVTOL

In this section we solve the exact lifting task for the coupled PVTOL with positive values of the parameter  $\epsilon_P$  and show that the lifted trajectory depends continuously on the parameter.

### 4.1 Trajectory lifting for the decoupled PVTOL model

The exact lifting task can be easily solved for the decoupled PVTOL model, that is for the model with  $\epsilon_P = 0$ . Since we will often refer to this special case, we use for it the ad hoc notation PVTOL<sub>0</sub>. In [15] the PVTOL<sub>0</sub> was shown to be input-output linearizable provided  $u_1 \neq 0$ . Here, we provide sufficient conditions to compute a trajectory of the system given a  $C^4$  desired output curve. We rewrite the equation for the PVTOL<sub>0</sub> since this will play an important role in the development of our strategy.

$$\begin{aligned} \ddot{y} &= u_1 \sin \varphi \\ \ddot{z} &= -u_1 \cos \varphi + g \\ \ddot{\varphi} &= u_2. \end{aligned} \quad (3)$$

The following assumption will be used in the paper.

**Assumption 4.1 (Annulus assumption)** Let  $\mathbf{y}_d(\cdot) \in \mathcal{C}^4$  be a desired output curve. Let  $\mathbf{a}_d(t) := (\ddot{y}_d(t), g - \ddot{z}_d(t))^T$ , assume that  $\mathbf{a}_d(t) \neq 0$  and  $0 < a_{\min} \leq \|\mathbf{a}_d\| \leq a_{\max}$  for all  $t$ .

A graphical interpretation of the annulus assumption is depicted in Figure 2. We ask the vector  $\mathbf{a}_d$  to lie in the annulus of radii  $a_{\min}$  and  $a_{\max}$  centered at the origin of the reference axes  $\vec{y}$  and  $\vec{z} - g$ .

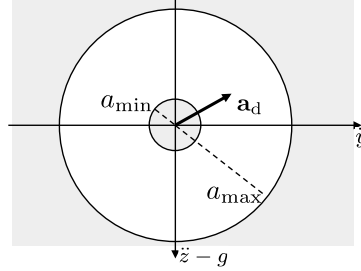


Fig. 2. Acceleration range

Under this assumption the (state-input) trajectory of the PVTOL<sub>0</sub> may be parametrized in terms of the desired output curve by

$$\begin{aligned} \varphi_0(t) &= \angle \mathbf{a}_d(t) = \text{atan2}(\ddot{y}_d(t), g - \ddot{z}_d(t)) \\ u_{10}(t) &= \|\mathbf{a}_d(t)\| = ((g - \ddot{z}_d(t))^2 + \ddot{y}_d^2(t))^{\frac{1}{2}} \\ u_{20}(t) &= \ddot{\varphi}_0(t). \end{aligned} \tag{4}$$

Equations in (4) allow to compute a trajectory of the PVTOL<sub>0</sub> for a given output curve satisfying the annulus assumption, thus exactly solving the trajectory lifting task (on any interval  $[0, T]$ ). This is a straightforward consequence of the input-output linearizability of PVTOL<sub>0</sub>.

#### 4.2 Trajectory lifting for the coupled PVTOL via dichotomy

Next, we prove that, given a desired output curve satisfying the annulus assumption, it exists a trajectory of the PVTOL exactly solving the lifting task for suitable positive values of the parameter  $\epsilon_P$  and, as  $\epsilon_P$  goes to zero, this trajectory depends continuously on it. To prove the result we use a feedback transformation that takes the system into the form of a *driven pushed pendulum* where the parameter  $\epsilon_P$  plays the role of the pendulum length. The result that we prove is based on and extends results in [14] on finding upright trajectories of an inverted pendulum.

Let us consider the feedback transformation given by

$$\begin{bmatrix} u_1 \\ \epsilon_P u_2 \end{bmatrix} = \begin{bmatrix} \sin \varphi & -\cos \varphi \\ -\cos \varphi & -\sin \varphi \end{bmatrix} \left( \begin{bmatrix} 0 \\ -g \end{bmatrix} + \begin{bmatrix} v_1 \\ v_2 \end{bmatrix} \right). \tag{5}$$

The dynamics of the system becomes

$$\begin{aligned} \ddot{y} &= v_1 \\ \ddot{z} &= v_2 \\ \epsilon_P \ddot{\varphi} &= (g - v_2) \sin \varphi - v_1 \cos \varphi. \end{aligned} \tag{6}$$

We have written the dynamics in a form that is somehow unusual, since the parameter  $\epsilon_P$  appears in the left hand side of the differential equation. This form has the advantage that it is well defined even for  $\epsilon_P = 0$ . In this case the model in (6) is defined by an algebraic differential equation. Also, to be consistent, we have to consider as control inputs  $u_1$  and  $\epsilon_P u_2$  and think of the roll dynamics in (1) as  $\epsilon_P \ddot{\varphi} = \epsilon_P u_2$ .

**Remark 4.2** *The feedback transformation highlights an important property of the coupled PVTOL ( $\epsilon_P \neq 0$ ), i.e., it has a well defined relative degree,  $r = [2, 2]$ , with respect to the output  $(y, z)$ . It is worth noting that for  $\epsilon_P > 0$  the zero dynamics of the system is unstable (the driven pendulum is pushed and thus inverted), and therefore the system is non-minimum phase. This is an interesting feature of the PVTOL that makes the lifting task more challenging.*

An important role in the study of the trajectory manifold of the PVTOL is played by the “quasi trajectory” that (with some abuse of notation) we call *quasi-static trajectory*. It is a time parametrized curve built pretending that, at each instant  $t$ , the roll angle assumes the equilibrium value obtained if  $\ddot{y}(t)$  and  $\ddot{z}(t)$  were constant. By imposing  $\ddot{\varphi} = 0$  in equation (6) we get

$$\tan \varphi_{qs}(t) = \frac{\ddot{y}(t)}{(g - \ddot{z}(t))}. \quad (7)$$

It is worth noting that the quasi-static roll trajectory does not depend on  $\epsilon_P$  and coincides with the roll trajectory that we obtained for the PVTOL<sub>0</sub> system. Also, in the driven pushed pendulum the quasi-static trajectory produces an acceleration vector  $\mathbf{a}_d$  aligned along the pendulum axis.

A first straightforward but interesting result can be proven. Before stating the proposition we need some more notation. Recall that in Section 2 we have written the PVTOL dynamics in state space form and denoted  $x$  and  $u$  the state and the input of the system. Consistently with that notation we let  $x$  be the state of system in (6) and  $v := (v_1, v_2)$ , so that  $\dot{x} = f_{\text{pend}}(x, v)$  with suitably defined  $f_{\text{pend}}$ .

**Proposition 4.3** *Let  $\mathbf{y}_d(\cdot)$  be a desired  $\mathcal{C}^4$  output curve on  $(-\infty, +\infty)$  satisfying the annulus assumption. Let  $(x^*(\cdot), u^*(\cdot))$  be the trajectory solving the exact lifting for the PVTOL<sub>0</sub> model in (3) according to (4) and  $(x_{\text{pend}}^*(\cdot), v_{\text{pend}}^*(\cdot))$  the trajectory solving the exact lifting for the model in (6) with  $\epsilon_P = 0$ . Then*

$$x^*(\cdot) = x_{\text{pend}}^*(\cdot)$$

and

$$u_1^*(\cdot) = (g - \ddot{z}_d(\cdot)) \cos \varphi^*(\cdot) + \ddot{y}_d(\cdot) \sin \varphi^*(\cdot),$$

consistently with equation (5).

With this feedback transformation in hand, the exact lifting task for the PVTOL can be formulated as follows. Given a desired output curve  $\mathbf{y}_d(\cdot)$ , find a bounded roll trajectory for the roll dynamics

$$\epsilon_P \ddot{\varphi} = (g - \ddot{z}_d(t)) \sin \varphi - \ddot{y}_d(t) \cos \varphi. \quad (8)$$

The proof of existence of  $\varphi_{\epsilon_P}(\cdot)$  and right continuity with respect to  $\epsilon_P$  is based on the presence of a dichotomy in the linearization of the dynamics of an inverted pendulum about the vertical position. In [14] a bounded trajectory of the inverted pendulum is proven to exist as a fixed point of a contraction mapping. Here, we generalize the result in [14] in the sense that we allow the acceleration of the pivot point to lie in the entire annulus (not only on the horizontal axis  $\ddot{z} = 0$ ) and we study the properties of the lifted trajectory when the parameter  $\epsilon_P$  (the length of the pendulum) goes to zero.

We rewrite the roll dynamics in (8) in the form

$$\epsilon_P \ddot{\varphi} = a_d(t) \sin(\varphi - \varphi_{qs}(t)), \quad (9)$$

where  $a_d(t) = \|\mathbf{a}_d(t)\|$ . Then we write it in terms of the error from the *quasi-static* angle,  $\theta = \varphi - \varphi_{qs}$ , as

$$\epsilon_P \ddot{\theta} = a_d(t) \sin \theta - \epsilon_P \ddot{\varphi}_{qs}(t), \quad (10)$$

and, in order to use dichotomy, in terms of its linearization about  $\theta = 0$ ,

$$\epsilon_P \ddot{\theta} = a_d(t) \theta - a_d(t) \left( \theta - \sin \theta + \epsilon_P \frac{\ddot{\varphi}_{qs}(t)}{a_d(t)} \right). \quad (11)$$

Let us consider the linear time-varying system driven by a bounded external input

$$\epsilon_P \ddot{\gamma} = a_d(t)\gamma - a_d(t)\mu(t).$$

In [14] it was proven that, for any  $\epsilon_P > 0$ , the undriven system admits an exponential dichotomy and, therefore that, working in a noncausal fashion, for any bounded input  $\mu(\cdot)$  a bounded solution  $\gamma(\cdot)$  exists. We let  $\mathcal{A}_{\epsilon_P} : L_\infty \rightarrow L_\infty$  be the linear map  $\mu(\cdot) \mapsto \gamma(\cdot)$ . The following holds.

**Lemma 4.4 (Theorem 5 in [14])** *For any  $\epsilon_P > 0$ ,  $\mathcal{A}_{\epsilon_P}$  is a bounded linear operator with  $\|\mathcal{A}_{\epsilon_P}\| = 1$ .*

Defining the nonlinear operator  $\mathcal{N}_{\epsilon_P}$  as

$$\theta \rightarrow \mathcal{A}_{\epsilon_P} \left[ \theta - \sin \theta + \epsilon_P \frac{\ddot{\varphi}_{qs}(t)}{a_d(t)} \right] =: \mathcal{N}_{\epsilon_P} [\theta(\cdot)],$$

Clearly, a bounded curve  $\theta(\cdot)$  is a solution of (10) if and only if it is a fixed point of  $\mathcal{N}_{\epsilon_P}$ , i.e.  $\theta(\cdot) = \mathcal{N}_{\epsilon_P} [\theta(\cdot)]$ .

We are now ready to prove the main result in this section. The proof relies on arguments of Theorem 8 in [14].

**Theorem 4.5** *Given a  $\mathcal{C}^4$  output curve  $(y(\cdot), z(\cdot))$  on  $(-\infty, +\infty)$ , with  $0 < a_{\min} \leq a_d(t) \leq a_{\max}$  for all  $t$  ( $\ddot{\varphi}_{qs}(\cdot)$  bounded), then there exists an  $\epsilon_{P0} > 0$ ,*

$$\epsilon_{P0} = \frac{1}{\|\ddot{\varphi}_{qs}(\cdot)/a_d(\cdot)\|_{L_\infty}},$$

*such that for any  $\epsilon_P \in (0, \epsilon_{P0})$*

- (i) *there exists a bounded trajectory  $\theta_{\epsilon_P}(\cdot)$  of (10) so that  $\varphi_{\epsilon_P}(\cdot) = \varphi_{qs}(\cdot) + \theta_{\epsilon_P}(\cdot)$  is a bounded trajectory of (8) whenever  $\varphi_{qs}(\cdot)$  is bounded. and*
- (ii)  *$\|\varphi_{\epsilon_P}(\cdot) - \varphi_{qs}(\cdot)\|_{L_\infty} \leq \sin^{-1} \frac{\epsilon_P}{\epsilon_{P0}}$ .*

*Proof:* In order to prove existence of the trajectory, we show that there exists  $\delta_0 > 0$  such that for any  $\delta \in (0, \delta_0)$  the map  $\mathcal{N}_{\epsilon_P}$  is a contraction on the invariant set  $\overline{B}_\delta = \{\theta(\cdot) \in L_\infty \mid \|\theta(\cdot)\|_{L_\infty} \leq \delta\}$ . The set  $\overline{B}_\delta$  is invariant if for any  $\delta$

$$\|\mathcal{N}_{\epsilon_P} [\theta(\cdot)]\|_{L_\infty} \leq \|\mathcal{A}_{\epsilon_P}\| \|\theta(\cdot) - \sin \theta(\cdot)\|_{L_\infty} + \epsilon_P \left\| \frac{\ddot{\varphi}_{qs}(\cdot)}{a_d(\cdot)} \right\|_{L_\infty} \leq \delta.$$

Recall that  $\|\mathcal{A}_{\epsilon_P}\| = 1$  for all  $\epsilon_P > 0$  and  $f(\delta) = \delta - \sin \delta$  is monotonically increasing on  $[0, \pi]$ . Therefore, posing  $\epsilon_{P0} = \frac{1}{\|\ddot{\varphi}_{qs}(\cdot)/a_d(\cdot)\|_{L_\infty}}$ ,  $\overline{B}_\delta$ ,  $\delta \in [0, \pi]$ , is invariant under  $\mathcal{N}_{\epsilon_P}$  if

$$\frac{\epsilon_P}{\epsilon_{P0}} \leq \sin \delta.$$

Now, the function  $f(\cdot)$  is Lipschitz continuous on  $[0, \delta_0] \subset [0, \pi]$  with Lipschitz constant  $1 - \cos \delta_0$ , i.e.  $|f(\delta_1) - f(\delta_2)| \leq (1 - \cos \delta_0)|\delta_1 - \delta_2|$  for all  $\delta_1, \delta_2 \in [0, \delta_0] \subset [0, \pi]$ . Therefore, choosing  $\delta < \pi/2$  and such that  $\sin \delta \geq \frac{\epsilon_P}{\epsilon_{P0}}$ , we have

$$\|\mathcal{N}_{\epsilon_P} [\theta_1(\cdot)] - \mathcal{N}_{\epsilon_P} [\theta_2(\cdot)]\|_{L_\infty} \leq \rho \|\theta_1(\cdot) - \theta_2(\cdot)\|_{L_\infty},$$

with  $\rho = 1 - \cos \delta < 1$ , so that  $\mathcal{N}_{\epsilon_P}$  is a contraction on the invariant set  $\overline{B}_\delta$ . In particular, the minimal set is obtained for  $\delta = \sin^{-1} \frac{\epsilon_P}{\epsilon_{P0}}$ . This gives the bound

$$\|\theta(\cdot)\|_{L_\infty} = \|\varphi_{\epsilon_P}(\cdot) - \varphi_{qs}(\cdot)\|_{L_\infty} \leq \sin^{-1} \frac{\epsilon_P}{\epsilon_{P0}}$$

proving statement (ii). ■

Next theorem follows easily from the results above.



**Theorem 4.6 (Exact lifting for the PVTOL)** *Let  $\mathbf{y}_d(t)$ ,  $t \in [0, T]$ , be a desired  $\mathcal{C}^4$  output curve for the PVTOL. Then there exists a trajectory  $(x^*(\cdot), u^*(\cdot))$ , with initial condition  $x_0 = x^*(0)$ , such that  $p(x^*(t)) = \mathbf{y}_d(t)$  for all  $t \in [0, T]$ .*

*Proof:* The external velocities are easily the derivatives of the desired outputs, while the roll and roll rate trajectories  $\phi^*(\cdot)$  and  $\dot{\phi}^*(\cdot)$  on  $[0, T]$  can be chosen as the restriction to  $[0, T]$  of the trajectories on the infinite horizon. These are proven to exist by Theorem 4.5. ■

## 5 Optimal control based strategy for feasible trajectory lifting

In this section we provide a strategy to solve the practical feasible trajectory lifting task. The idea is to attack the problem by means of optimal control combined with continuation and relaxation methods.

Let  $\xi = (x(t), u(t))$ ,  $t \in [0, T]$ , be a state-input curve. If  $(x(t), u(t)) \in \overline{\mathcal{XU}}$  for almost all  $t \in [0, T]$ , we say that  $\xi$  is a feasible curve and write  $\xi \in \overline{\mathcal{XU}}$ . Proceeding formally, to solve the practical feasible lifting task in Definition 3.5, we should solve the following optimal control problem

$$\begin{aligned} & \min_{\xi \in \mathcal{T}} \|p(x(\cdot)) - \mathbf{y}_d(\cdot)\|_{L_2} \\ & \text{subj. to } \xi \in \overline{\mathcal{XU}}. \end{aligned}$$

The main idea behind our strategy is not to attack the constrained lifting problem directly, but to embed it into a family of relaxed problems and use continuation with respect to parameters to find a solution. Informally, we perform the following steps: (i) embed the maneuvering system into a family of systems, (ii) design a routine to solve the unconstrained lifting task for a fixed embedding system in order to obtain a desired (state-input) trajectory  $\xi_d$ , (iii) minimize a weighted  $L_2$  distance from the infeasible unconstrained lifted trajectory,  $\xi_d$ , over the feasible trajectories, (iv) relax the constrained optimal control problem and design a solver for the relaxed problem (for each fixed embedding system), and (v) design an update policy for the system and problem parameters.

### Embedding systems

We embed the maneuvering system into a family of systems with the property that, for some choice of the parameters, the system has a “special” structure. That is, there exist values of the parameters for which the (unconstrained) lifting task can be solved more easily (e.g. because the system is differentially flat or has some “nice” geometry). As regards the PVTOL, we consider the family of PVTOL models parametrized by the coupling parameter  $\epsilon_P$  with  $\epsilon_P \geq 0$ . From the results in the previous section we know that we can easily solve the unconstrained lifting task for the decoupled system, i.e. for  $\epsilon_P = 0$ , and that an unconstrained trajectory is proved to exist for some positive values of the parameter.

### Unconstrained lifting

The objective of this step is to obtain a (state-input) trajectory solving the unconstrained lifting task to use as the desired curve for the constrained problem. We use a *dynamic embedding* technique introduced in [13]. Informally, it consists of embedding the original system into a fully controllable system and solve the practical trajectory lifting by penalizing the *embedding input* much more than the real ones. We describe an ad-hoc version of this technique for the PVTOL, but it can be easily generalized to other maneuvering systems.

First, observe that for  $\epsilon_P = 0$  a lifted trajectory of the PVTOL can be easily obtained by equations in (4). For  $\epsilon_P > 0$  we know by Theorem 4.5 that, under suitable conditions on  $\mathbf{y}_d(\cdot)$ , there exists a trajectory (on the infinite time horizon) solving the exact lifting task, and it depends continuously on  $\epsilon_P$ . An approximation of this trajectory on the finite horizon can be computed in three steps: (i) compute the external position and velocities trajectories, (ii) compute the internal trajectories, (iii) compute the input trajectories. The first step is straightforward. The external position trajectories are simply given by the desired curves and the velocities are obtained by differentiation. The input trajectories can be easily computed by equation (5) once the trajectory of the internal position state (the roll trajectory) is known. Thus, the dynamic embedding technique is applied to compute the roll and roll rate trajectories. We use the dynamics in the new coordinates (6) and find a trajectory of the reduced system in (8). We embed the roll dynamics into the driven system

$$\epsilon_P \ddot{\varphi} = (g - \ddot{z}_d(t)) \sin \varphi - \ddot{y}_d(t) \cos \varphi + \epsilon_P u_{\text{emb}}, \quad (12)$$

where  $u_{\text{emb}}$  is the embedding input used to drive the system along any desired admissible trajectory. If we rewrite (12) in state space form as  $\dot{x}_\varphi = f_\varphi(t, x_\varphi, u_{\text{ext}})$ , where  $x_\varphi = (\varphi, \dot{\varphi})$  and  $x_{qs} = (\varphi_{qs}, \dot{\varphi}_{qs})$ , the following optimization problem may be posed

$$\begin{aligned} & \text{minimize } \frac{1}{2} \int_0^T \|x_\varphi(\tau) - x_{qs}(\tau)\|_{Q_\varphi}^2 d\tau + r |u_{\text{emb}}(\tau)|^2 d\tau + \frac{1}{2} \|x_\varphi(T) - x_{qs}(T)\|_{P_\varphi}^2 \\ & \text{subject to } \dot{x}_\varphi = f_\varphi(t, x_\varphi, u_{\text{emb}}), \quad x_\varphi(0) = x_{qs}(0). \end{aligned} \quad (13)$$

where we use the *quasi-static* trajectory as a desired curve to find the actual trajectory,  $Q_\varphi > 0$  and  $P_\varphi > 0$  are positive definite weighting matrices and  $r > 0$  is the weight of the embedding input. Using a sufficiently high weight  $r$  for the embedding input, we obtain a trajectory arbitrarily close to the exact lifted trajectory. The optimization problem is solved by using the projection operator based Newton method described in Appendix A.

We denote  $\text{LIFT}_{\epsilon_P}$  the routine described above to solve the unconstrained lifting. Specifically, we let  $\xi = \text{LIFT}_{\epsilon_P}(\xi_0; \mathbf{y}_d(\cdot))$  be a trajectory solving the practical lifting task for the desired output curve  $\mathbf{y}_d(\cdot)$  and computed by using  $\xi_0$  as initial guess. The routine is parametrized by the coupling parameter  $\epsilon_P$  of the PVTOL dynamics. For  $\epsilon_P = 0$  the lifting procedure does not need any initial guess. Thus, we simply write  $\xi = \text{LIFT}_0(\mathbf{y}_d(\cdot))$ .

#### Constrained $L_2$ distance minimization and optimal control relaxation

With a full unconstrained trajectory  $\xi_d = (x_d(\cdot), u_d(\cdot))$  in hand, we can pose the following constrained optimal control problem, where we minimize a weighed  $L_2$  distance from  $\xi_d$  subject to feasibility,

$$\begin{aligned} & \min_{(x(\cdot), u(\cdot))} \frac{1}{2} \int_0^T \|x(\tau) - x_d(\tau)\|_Q^2 + \frac{1}{2} \|u(\tau) - u_d(\tau)\|_R^2 d\tau + \frac{1}{2} \|x(T) - x_d(T)\|_{P_f}^2 \\ & \text{subj. to } \dot{x}(t) = f(x(t), u(t)), \quad x(0) = x_0 \\ & \quad (x(t), u(t)) \in \overline{\mathcal{XU}}, \quad \text{for a.a. } t \in [0, T] \end{aligned}$$

where  $Q$ ,  $R$  and  $P_f$  are positive definite matrices. The idea is to choose  $Q$ ,  $R$  and  $P_f$  so that the weights associated to the outputs (external position states) are much larger than the weights of the other states and the inputs. Denoting  $\|\xi - \xi_d\|_{L_2} := \frac{1}{2} \int_0^T \|x(\tau) - x_d(\tau)\|_Q^2 + \|u(\tau) - u_d(\tau)\|_R^2 d\tau + \frac{1}{2} \|x(T) - x_d(T)\|_{P_f}^2$ , we can rewrite the problem in a more compact notation as

$$\begin{aligned} & \min_{\xi \in \mathcal{T}_{\epsilon_P}} \|\xi - \xi_d\|_{L_2} \\ & \text{subj. to } \xi \in \overline{\mathcal{XU}}, \end{aligned} \quad (14)$$

where we have denoted  $\mathcal{T}_{\epsilon_P}$  the trajectory manifold for a given value of the parameter  $\epsilon_P$ .

Now, we introduce a relaxed version of the above optimal control problem. To do that, we first define a relaxed version of the feasibility region. That is, we parametrize the feasibility region by means of a scaling factor  $\rho \in [0, 1]$  that allows to enlarge the nominal region up to a larger one containing the unconstrained lifted trajectory  $\xi_d$ .

**Definition 5.1 (Scalable feasibility region)** *A scalable feasibility region is defined as*

$$\overline{\mathcal{XU}}_\rho = \{(x, u) \in \mathbb{R}^n \times \mathbb{R}^m \mid c_j(x, u; \rho) \leq 0, \rho \in [0, 1], j \in \{1, \dots, k\}\}$$

such that

- (i)  $c_j(x, u; \rho)$ ,  $j \in \{1, \dots, k\}$ , is  $\mathcal{C}^2$  in  $x$  and  $u$  and varies smoothly with  $\rho$ .
- (ii) for any  $\rho \in [0, 1]$ ,  $\mathcal{XU}_\rho$ , the interior of  $\overline{\mathcal{XU}}_\rho$ , is a nonempty simply connected set.
- (iii) for any  $0 < \rho_1 < \rho_2$ ,  $\mathcal{XU}_{\rho_1} \supset \mathcal{XU}_{\rho_2}$ ;
- (iv) the projection of  $\mathcal{XU}_\rho$  on the input space  $\pi_u \mathcal{XU}_\rho = \{u \in \mathbb{R}^m \mid (x, u) \in \mathcal{XU}_\rho \forall \text{ fixed } x\}$  is convex;
- (v) for every desired output trajectory  $\mathbf{y}_d(\cdot)$ , the lifted trajectory  $\xi_d = (x_d(\cdot), u_d(\cdot))$  (if it exists) is such that  $\exists \rho_0 \in [0, 1]$  such that  $(x_d(t), u_d(t)) \in \mathcal{XU}_{\rho_0}$  for every  $t \in [0, T]$ .

With this definition in hand we can introduce the relaxed version of the optimal control problem in (14). We use the barrier functional idea described in Appendix A. Namely, we add to the cost functional a barrier term to enforce feasibility with respect to the point-wise constraints. Thus, the optimal control problem relaxation is given by

$$\min_{\xi \in \mathcal{T}_{\epsilon_P}} \|\xi - \xi_d\|_{L_2} + \epsilon_c b_{\delta_c, \rho}(\xi) \quad (15)$$

where  $\mathcal{T}_{\epsilon_P}$  is the trajectory manifold for a given value of  $\epsilon_P$  and  $b_{\delta_c, \rho}(\xi)$  is a barrier functional defined consistently with (A.3). It is worth noting that here the barrier functional is parametrized also by  $\rho$  because the constraints are. The relaxed optimal control problem is solved by using the projection operator Newton method in Appendix A.

Next, we introduce some useful notation. For a given scalable feasibility region  $\mathcal{XU}_\rho$ , parametrized by  $\rho$ , we denote  $\text{PO\_Newt}_{\epsilon_P}(\xi_d, \xi_0; \epsilon_c, \rho)$  a routine that takes as inputs a desired (state-control) curve  $\xi_d$  and an initial trajectory  $\xi_0$ , and computes a feasible trajectory  $\xi \in \mathcal{T}_{\epsilon_P}$ , with  $\xi \in \mathcal{XU}_\rho$ , by solving the nonlinear optimal control relaxation in (15). The routine is parametrized by the embedding parameter  $\epsilon_P$  (the coupling parameter for the PVTOL), the parameter  $\epsilon_c$  scaling the barrier functional (see Appendix A.3) and the parameter  $\rho$  scaling the feasibility region.

We are now ready to define our strategy. First, we provide an informal description. From now on we call *unconstrained lifted trajectory* a trajectory solving the practical (unconstrained) lifting task.

*Lift and Constrain Strategy:* The strategy consists of the following steps: (i) given a desired output curve  $\mathbf{y}_d(\cdot)$ , an unconstrained lifted trajectory for an initial embedding system is computed (e.g., for the decoupled PVTOL with  $\epsilon_P = 0$ ); (ii) a continuation update on the parameter  $\epsilon_P$  is applied up to the nominal value  $\epsilon_P^{\text{nom}}$ ; (iii) a relaxed optimal control problem is solved for  $\rho = 0$  (feasibility region containing the lifted trajectory) and  $\epsilon_c = \epsilon_{c0}$  (for a suitable  $\epsilon_{c0} > 0$ ); (iv) a continuation update on the parameter  $\rho$  is applied shrinking the feasibility region up to its nominal value for  $\rho = 1$ ; (v) a continuation update on the parameter  $\epsilon_c$  is applied to regulate the closeness of the feasible trajectory from the boundary ( $\epsilon_c \rightarrow \epsilon_{ce}$  for some  $\epsilon_{ce}$ ).

Next we give a pseudo-code description of the strategy.

<b>Strategy:</b>	Lift and Constrain Strategy
<b>Task:</b>	Feasible trajectory lifting
<b>Inputs:</b>	$\epsilon_P^{\text{nom}}, \overline{\mathcal{XU}}, \mathbf{y}_d(\cdot), \epsilon_{ce}$
<b>Output:</b>	$\xi_c \in \mathcal{T}_{\epsilon_P^{\text{nom}}}$ with $\xi_c \in \mathcal{XU}$
<b>Parameters:</b>	$(\epsilon_P, \epsilon_c, \rho) \in \mathbb{R}_{\geq 0}^3$ $(\xi_d, \xi_c) \in \mathcal{T}_{\epsilon_P} \times \mathcal{T}_{\epsilon_P}$
<b>Initialization:</b>	$\epsilon_P := 0, \epsilon_c := \epsilon_{c0}, \rho := 0$ $\xi_d := \text{LIFT}_0(\mathbf{y}_d(\cdot))$ $\xi_c := \xi_d$
1. <b>WHILE</b> $\epsilon_P < \epsilon_P^{\text{nom}}$ <b>DO</b> increase $\epsilon_P$ $\xi_d = \text{LIFT}_{\epsilon_P}(\xi_d; \mathbf{y}_d(\cdot))$ <b>END</b> 2. <b>WHILE</b> $\rho < 1$ <b>DO</b> increase $\rho$ $\xi_c = \text{PO\_Newt}_{\epsilon_P}(\xi_d, \xi_c; \epsilon_c, \rho)$ <b>END</b> 3. <b>WHILE</b> $\epsilon_c > \epsilon_{ce}$ <b>DO</b> decrease $\epsilon_c$ $\xi_c = \text{PO\_Newt}_{\epsilon_P}(\xi_d, \xi_c; \epsilon_c, \rho)$ <b>END</b> 4. <b>RETURN</b> $\xi_c$	

**Remark 5.2 (Variations of the strategy)** *Other variations of the above strategy can be obtained by changing the order of or combining the update steps of some parameters in the continuation strategy. These different choices can be thought as degrees of freedom in the designer's hands and their effectiveness is strongly related to the system dynamics and to the feasibility constraints.*

## 6 Strategy analysis

In this section we prove that under suitable conditions on the feasibility region we can find a feasible trajectory that solves locally the practical lifting task in Definition 3.6.

### 6.1 Differentiability of an optimal control minimizer with respect to parameters

We start providing a supporting result to prove the existence of a feasible trajectory. Namely, we prove, under suitable conditions, continuity and differentiability of an optimal control minimizer with respect to parameters. We present this result in a separate subsection for two reasons. First, this is the most subtle part to prove the existence of a feasible trajectory. Second, we believe this is an important stand alone result.

We consider an optimal control problem where the cost functional depends smoothly on a finite dimensional parameter and the system is independent of the parameter. In this section, we will refer to this parameter as  $\rho \in \mathbb{R}^p$ . This parameter may include, for instance, the scalar parameter  $\rho$  used for specifying the size of the feasible region as well as the scalar parameter  $\epsilon_c$  used in determining strictly feasible trajectories. We thus write the minimization problem

$$\min_{\xi \in \mathcal{T}} h(\xi, \rho).$$

Using Lemma A.2 in Appendix A, we can look for an unconstrained local minimum of the functional

$$g_\rho(\xi) = h(\mathcal{P}(\xi), \rho).$$

We will suppose that the scaling and offset of the parameters have been chosen in such a manner that the nominal value of the parameter vector is  $\rho = 0$ .

**Remark 6.1 (Parametrization with respect to system parameters)** *The parameter  $\rho$  does not include the system parameter  $\epsilon_p$ . Indeed, the parameter  $\epsilon_p$  affects the dynamics and, thus, the projection operator  $\mathcal{P}$ . The following results hold true for the case where also the projection operator depends on the parameter, i.e.  $g_\rho(\xi) = h(\mathcal{P}(\xi, \rho), \rho)$ , provided the projection operator is shown to depend smoothly on the system parameter.*

Let  $\xi_0 \in \mathcal{T}$  and consider the nature of  $g_0(\xi)$  on a neighborhood of  $\xi_0$ . In particular, we consider  $\xi$  of the form  $\xi_0 + \zeta$  where  $\|\zeta\| < \delta$  and  $\delta > 0$  is such that  $\xi_0 + \zeta \in \text{dom } \mathcal{P}$  for each such  $\zeta$ . For  $\mathcal{C}^2$   $g_0(\cdot)$ , we have

$$g_0(\xi_0 + \zeta) = g_0(\xi_0) + Dg_0(\xi_0) \cdot \zeta + \frac{1}{2} D^2 g_0(\xi_0) \cdot (\zeta, \zeta) + r(\xi_0, \zeta) \cdot (\zeta, \zeta) \quad (16)$$

where the remainder satisfies

$$|r(\xi_0, \zeta) \cdot (\zeta, \zeta)| / \|\zeta\|^2 \rightarrow 0 \quad \text{as} \quad \|\zeta\| \rightarrow 0 \quad (17)$$

where  $\|\cdot\|$  is the  $L_\infty$  norm. Using the  $\mathcal{C}^2$  identity

$$\phi(1) = \phi(0) + \phi'(0) + \int_0^1 (1-s) \phi''(s) ds$$

together with  $\phi(s) = g_0(\xi_0 + s\zeta)$ , we obtain the explicit expression

$$r(\xi_0, \zeta) \cdot (\zeta_1, \zeta_2) = \int_0^1 (1-s) [D^2 g_0(\xi_0 + s\zeta) - D^2 g_0(\xi_0)] ds \cdot (\zeta_1, \zeta_2) \quad (18)$$

which has been slightly generalized to depend on three, possibly independent, perturbations. Using the fact that  $D^2 g_0(\cdot)$  is continuous as a mapping from the trajectory manifold  $\mathcal{T}$  to set of continuous bilinear functionals on  $L_\infty$ ,

we easily verify that the remainder  $r(\xi_0, \zeta) \cdot (\zeta, \zeta)$  defined by (18) satisfies, as it *must*, the higher order property (17). Equations (16), (18) provide a *second order expansion with remainder* formula for the  $\mathcal{C}^2$  mapping  $g_0(\cdot)$ , valid in an  $L_\infty$  neighborhood of any  $\xi_0 \in \mathcal{T}$ . In fact, the formula given by (16), (18) is somewhat more general, requiring only that  $\xi_0 \in L_\infty$  and  $\delta > 0$  are such that  $B_\delta(\xi_0) \subset \text{dom } \mathcal{P}$ .

Now, since the functional  $g_0(\cdot)$  is the composition of an integral functional and a projection operator, from [10] the value of the bilinear expression  $D^2g_0(\xi) \cdot (\zeta_1, \zeta_2)$  for  $\xi \in \text{dom } \mathcal{P}$  and  $\zeta_i \in L_\infty$  is of the form

$$D^2g_0(\xi) \cdot (\zeta_1, \zeta_2) = \int_0^T \gamma_1(\tau)^T W(\tau) \gamma_2(\tau) d\tau + (\pi_1 \gamma_1(T))^T P_f (\pi_1 \gamma_2(T)),$$

where  $\gamma_i = D\mathcal{P}(\xi) \cdot \zeta_i$  and where  $P_f = P_f^T \in \mathbb{R}^{n \times n}$  and the bounded matrix  $W(t) = W(t)^T \in \mathbb{R}^{n \times n}$ ,  $t \in [0, T]$ , depend continuously on  $\eta = \mathcal{P}(\xi)$ , hence continuously on  $\xi$ . Using these facts, we see that

**Lemma 6.2** *Let  $\xi_0 \in \mathcal{T}$  and suppose that  $\delta > 0$  is such that  $B_\delta(\xi_0) \subset \text{dom } \mathcal{P}$ . Then, there is a nondecreasing function  $\bar{r}(\cdot)$  with  $\bar{r}(0) = 0$  such that*

$$|r(\xi_0, \zeta) \cdot (\zeta_1, \zeta_2)| \leq \bar{r}(\|\zeta\|) \|\zeta_1\|_{L_2} \|\zeta_2\|_{L_2} \quad (19)$$

for all  $\zeta, \zeta_1, \zeta_2 \in B_\delta$ .

*Proof:* Since  $\mathcal{P}$  is  $\mathcal{C}^2$ ,  $D\mathcal{P}(\xi)$  is a continuous linear projection operator with respect to the  $L_\infty$  norm. Using an explicit formula for  $D\mathcal{P}(\xi) \cdot \zeta$ , it can be shown, [10], that  $D\mathcal{P}(\xi)$  may be extended to a linear projection operator  $D\mathcal{P}(\xi)_{L_2}$  on  $L_2$  that is continuous with respect to the  $L_2$  norm. The result follows easily using (18). ■

Suppose now that  $\xi_0 \in \mathcal{T}$  is a stationary trajectory of  $g_0(\cdot)$  so that  $Dg_0(\xi_0) \cdot \zeta = 0$  for all  $\zeta \in L_\infty$  and that  $\delta > 0$  is such that  $B_\delta(\xi_0) \subset \text{dom } \mathcal{P}$ . It follows that

$$g_0(\xi_0 + \zeta) \geq g_0(\xi_0) + \frac{1}{2} D^2g_0(\xi_0) \cdot (\zeta, \zeta) - \bar{r}(\|\zeta\|) \|\zeta\|_{L_2}^2 \quad (20)$$

for all  $\|\zeta\| < \delta$  where  $\bar{r}(\cdot)$  is given by Lemma 6.2. Restricting (20) to  $\zeta \in T_{\xi_0} \mathcal{T}$ , we obtain the fundamental second order sufficient condition (SSC) for  $\xi_0$  to be an isolated local minimizer.

**Theorem 6.3** *Suppose  $\xi_0 \in \mathcal{T}$  is such that  $Dg_0(\xi_0) \cdot \zeta = 0$  for all  $\zeta \in L_\infty$  and that there is a  $c_0 > 0$  such that*

$$D^2g_0(\xi_0) \cdot (\zeta, \zeta) \geq c_0 \|\zeta\|_{L_2}^2 \quad \text{for all } \zeta \in T_{\xi_0} \mathcal{T}. \quad (21)$$

*Then  $\xi_0$  is an isolated local minimizer in the sense that there is a  $\delta > 0$  such that*

$$g_0(\xi_0) < g_0(\xi)$$

*for all  $\xi \in \mathcal{T}$  with  $\|\xi - \xi_0\| < \delta$ ,  $\xi \neq \xi_0$ .*

*Proof:* Taking  $\delta_1 > 0$  be such that  $\bar{r}(\delta_1) < c_0/4$ , we find that  $g_0(\xi_0 + \zeta) \geq g_0(\xi_0) + (c_0/4) \|\zeta\|_{L_2}^2$  for all  $\zeta \in T_{\xi_0} \mathcal{T}$  with  $\|\zeta\| < \delta_1$ . By Theorem A.1, each  $\xi \in \mathcal{T}$  near  $\xi_0$  can be represented by a unique  $\zeta \in T_{\xi_0} \mathcal{T}$  according to  $\xi = \mathcal{P}(\xi_0 + \zeta)$  and the mapping  $\xi \mapsto \zeta$  is continuous. Thus there is a  $\delta < \delta_1$  such that  $\|\xi - \xi_0\| < \delta$  implies that  $\|\zeta\| < \delta_1$ . The result follows. ■

We call a local minimizer  $\xi_0 \in \mathcal{T}$  satisfying (21) a *second order sufficient condition local minimizer*, SSC local minimizer for short. According to Theorem 6.3, *every* SSC local minimizer is an *isolated* local minimizer. We also note that, in words, the condition (21) says that the quadratic functional  $\zeta \mapsto D^2g_0(\xi_0) \cdot (\zeta, \zeta)$  is *strongly positive* on the subspace  $T_{\xi_0} \mathcal{T}$ .

Consider now the (local) minimization of  $g_\rho(\xi)$  as the parameter  $\rho$  is varied on a neighborhood of  $\rho = 0$  where  $\xi_0$  is known to be an SSC local minimizer of  $g_0(\xi)$ . Since  $D^2g_\rho(\xi)$  is continuous in both  $\xi$  and  $\rho$ , we expect that, for each

sufficiently small  $\rho$ , there will be a corresponding SSC local minimizer  $\xi_\rho$  near  $\xi_0$  and that the mapping  $\rho \mapsto \xi_\rho$  will be continuous, and perhaps differentiable. The key idea is to use an appropriate implicit function theorem (IFT) to solve the first order necessary condition equation

$$Dg_\rho(\xi_\rho) = 0 \quad (22)$$

for  $\xi_\rho$  as a function of  $\rho$  starting from  $\xi_0$  at  $\rho = 0$ . Proceeding formally, we differentiate (22) with respect to  $\rho$  to obtain

$$\frac{\partial}{\partial \rho} Dg_\rho(\xi_\rho) + D\{Dg_\rho(\xi_\rho)\} \cdot \xi'_\rho = 0.$$

Thus, the derivative of  $\xi_\rho$  with respect to  $\rho$ ,  $\xi'_\rho$ , if it exists, is given formally by

$$\xi'_\rho = -[D\{Dg_\rho(\xi_\rho)\}]^{-1} \cdot \frac{\partial}{\partial \rho} Dg_\rho(\xi_\rho).$$

In this case, we expect that there is an implicit function theorem that says something like, if  $D\{Dg_\rho(\xi_\rho)\}$  is invertible at  $\rho = 0$ , then there is a neighborhood of  $\rho = 0$  on which  $\rho \mapsto \xi_\rho$  is well defined and  $\mathcal{C}^1$ . In what sense should the operator  $D\{Dg_0(\xi_0)\}$  be invertible and how can it be ensured? It turns out that the appropriate condition is that  $D^2g_0(\xi_0)$  be strongly positive on  $T_{\xi_0}\mathcal{T}$ , i.e., that it satisfy (21).

**Theorem 6.4** *Suppose that  $\xi_0 \in \mathcal{T}$  is an SSC local minimizer of  $g_0(\xi)$ . Then, there is a  $\delta > 0$  such that, for each  $\rho$  such that  $\|\rho\| < \delta$ , there is a local SSC minimizer  $\xi_\rho$  of  $g_\rho(\xi)$  near  $\xi_0$ . Furthermore  $\rho \mapsto \xi_\rho$  is continuously differentiable.*

*Proof:* The key is to show that, for  $\rho$  sufficiently small, we can compute a  $\xi \in \mathcal{T}$  such that  $Dg_\rho(\xi) \cdot \zeta = 0$  for all  $\zeta \in L_\infty$ . Using again Theorem A.1, we proceed by parametrizing  $\xi \in \mathcal{T}$  locally by  $\gamma \in T_{\xi_0}\mathcal{T}$  according to  $\xi = \mathcal{P}(\xi_0 + \gamma)$  and searching over  $\gamma$ . As in the proof of many IFTs, we solve for the desired  $\gamma$  using a contraction mapping. For simplicity, we will denote  $T_{\xi_0}\mathcal{T}$  by  $X$  so that we search for  $\gamma \in X$  such that  $Dg_\rho(\mathcal{P}(\xi_0 + \gamma)) \cdot \zeta = 0$  for all  $\zeta \in L_\infty$ .

First, note that, since  $D^2g_0(\xi_0)$  is strongly positive on  $X$ , the well-defined quadratic minimization problem

$$\lambda = \arg \min_{\zeta \in X} -\omega \cdot \zeta + \frac{1}{2} D^2g_0(\xi_0) \cdot (\zeta, \zeta)$$

defines a linear mapping  $\mathcal{S} : \omega \mapsto \lambda : \text{dom } \mathcal{S} \subset X^* \rightarrow X$  for some continuous linear functionals  $\omega \in X^*$ . The linear mapping  $\mathcal{S}$  provides the solution  $\lambda \in X$  to the functional equation

$$D^2g_0(\xi_0) \cdot (\lambda, \zeta) = \omega \cdot \zeta, \quad \zeta \in X,$$

effectively providing an inverse to the operator  $D\{Dg_0(\xi_0)\}$  formally described above. We will see that the functionals  $\omega \in X^*$  of interest belong to the domain of  $\mathcal{S}$ .

Define  $\mathcal{F}_\rho : X \rightarrow X^*$  by

$$\mathcal{F}_\rho(\gamma) \cdot \zeta = D^2g_0(\xi_0) \cdot (\gamma, \zeta) - Dg_\rho(\xi_0 + \gamma) \cdot \zeta$$

for all  $\zeta \in X$ . Note that  $\mathcal{F}_\rho(\gamma) \cdot \zeta$  is of the form

$$\mathcal{F}_\rho(\gamma) \cdot \zeta = \int_0^T a(\tau)^T z(\tau) + b(\tau)^T v(\tau) d\tau + r_1^T z(T)$$

for  $\zeta = (z(\cdot), v(\cdot)) \in X$  where  $a(\cdot)$ ,  $b(\cdot)$ , and  $r_1$  depend smoothly on the data  $\rho$  and  $\gamma$ . It follows that  $\mathcal{F}_\rho(\gamma) \in \text{dom } \mathcal{S} \subset X^*$ . A straightforward calculation shows that

$$\mathcal{G}_\rho(\gamma) = \mathcal{S} \cdot \mathcal{F}_\rho(\gamma)$$

defines a continuous operator  $\mathcal{G}_\rho : X \rightarrow X$  that is also continuous in  $\rho$ .

Note that, if  $\gamma \in X$  is a fixed point of  $\mathcal{G}_\rho(\cdot)$ ,  $\gamma = \mathcal{G}_\rho(\gamma)$ , then  $Dg_\rho(\xi_0 + \gamma) \cdot \zeta = 0$  for all  $\zeta \in X$ . This will imply that  $Dg_\rho(\xi_0 + \gamma) \cdot \zeta = 0$  for all  $\zeta \in L_\infty$  provided that  $\mathcal{P}(\xi_0 + \gamma)$  is sufficiently near  $\xi_0$ . In that case, we conclude that  $\xi_\rho = \mathcal{P}(\xi_0 + \gamma)$ . Also, for  $\rho = 0$ , we see that  $\gamma = 0$  is the fixed point,  $\mathcal{G}_0(0) = 0$  as expected.

We will show that, for  $\rho$  sufficiently small,  $\mathcal{G}_\rho(\cdot)$  is a contraction mapping with a unique fixed point. For  $\rho = 0$ , noting that  $Dg_\rho(\xi_0 + \gamma) \cdot (\cdot) = D^2g_0(\xi_0) \cdot (\gamma, \cdot) + o(\|\gamma\|)$ , we see that

$$\mathcal{G}_0(\gamma) = \mathcal{S} \cdot (D^2g_0(\xi_0) \cdot (\gamma, \cdot) - Dg_\rho(\xi_0 + \gamma) \cdot (\cdot)) = o(\|\gamma\|)$$

where we have used the fact that  $\mathcal{S}$  is continuous (bounded) on the elements of  $X^*$  of the noted form. By continuity in  $\rho$ , we see that there exist  $\rho_1, \delta > 0$  such that

$$\|\mathcal{G}_\rho(\gamma)\| \leq \delta$$

whenever  $\|\rho\| \leq \rho_1$  and  $\|\gamma\| \leq \delta$ . Now, fixing  $\rho$ ,  $\|\rho\| \leq \rho_1$ ,

$$\begin{aligned} \mathcal{G}_\rho(\gamma_1) - \mathcal{G}_\rho(\gamma_2) &= \mathcal{S} \cdot [Dg_\rho(\xi_0 + \gamma_2) \cdot (\cdot) - Dg_\rho(\xi_0 + \gamma_1) \cdot (\cdot)] \\ &= \mathcal{S} \cdot \left[ \int_0^1 D^2g_\rho(\xi_0 + \gamma_1 + s(\gamma_2 - \gamma_1)) ds \cdot (\gamma_2 - \gamma_1, \cdot) \right] \end{aligned}$$

so that there is a  $k < \infty$  such that

$$\|\mathcal{G}_\rho(\gamma_1) - \mathcal{G}_\rho(\gamma_2)\| \leq k\delta\|\gamma_1 - \gamma_2\|$$

for  $\|\gamma_1\| \leq \delta$  and  $\|\gamma_2\| \leq \delta$ . Shrinking  $\delta$ , if necessary, so that  $k\delta \leq 1/2$ , we see that  $\mathcal{G}_\rho$  is a contraction with unique fixed point  $\gamma_\rho$ .

To see that  $\rho \mapsto \gamma_\rho$  is continuous, write

$$\begin{aligned} \|\gamma_{\rho_1} - \gamma_{\rho_2}\| &= \|\mathcal{G}_{\rho_1}(\gamma_{\rho_1}) - \mathcal{G}_{\rho_2}(\gamma_{\rho_2})\| \\ &\leq \|\mathcal{G}_{\rho_1}(\gamma_{\rho_1}) - \mathcal{G}_{\rho_1}(\gamma_{\rho_2})\| + \|\mathcal{G}_{\rho_1}(\gamma_{\rho_2}) - \mathcal{G}_{\rho_2}(\gamma_{\rho_2})\| \\ &\leq (1/2)\|\gamma_{\rho_1} - \gamma_{\rho_2}\| + \|\mathcal{G}_{\rho_1}(\gamma_{\rho_2}) - \mathcal{G}_{\rho_2}(\gamma_{\rho_2})\| \end{aligned}$$

so that

$$\|\gamma_{\rho_1} - \gamma_{\rho_2}\| \leq 2\|\mathcal{G}_{\rho_1}(\gamma_{\rho_2}) - \mathcal{G}_{\rho_2}(\gamma_{\rho_2})\|$$

showing that  $\rho \mapsto \gamma_\rho$  is continuous since  $\rho \mapsto \mathcal{G}_\rho(\gamma)$  is continuous (for fixed  $\gamma$ ).

Differentiability is proven following standard arguments from implicit function theorems applied to  $\mathcal{G}_\rho$ . See, e.g., the second part of the proof of Theorem 4.E in [31].  $\blacksquare$

## 6.2 Existence of a feasible lifted trajectory

With the continuity result of the previous subsection in hands, we can prove our existence result. For a general maneuvering system we make the following standing assumption.

**Assumption 6.5** *Let  $\mathbf{y}_d(t)$ ,  $t \in [0, T]$ , be a given desired output curve. There exists a (state-input) trajectory  $\xi_d = (x_d(\cdot), u_d(\cdot)) \in \mathcal{T}$  on  $[0, T]$ , such that  $p(x_d(t)) = \mathbf{y}_d(t)$  for all  $t \in [0, T]$ .*

Formally, we state our main result in the next theorem.

**Theorem 6.6 (Existence of a feasible lifted trajectory)** *Let  $\mathbf{y}_d(t)$ ,  $t \in [0, T]$ , be a desired sufficiently smooth output curve satisfying Assumption 6.5 and  $\overline{\mathcal{XU}} \subset \mathbb{R}^n \times \mathbb{R}^m$  a compact feasibility region. Then, the following holds*

(i) for a given  $\delta_c > 0$ , there exist  $\rho_0 > 0$  and  $\epsilon_{c0} > 0$  such that the problem

$$\min_{\xi \in \mathcal{T}} \|\xi - \xi_d\|_{L_2} + \epsilon_c b_{\delta_c, \rho}(\xi), \quad (23)$$

has an isolated local minimizer for all  $0 \leq \rho < \rho_0$  and  $0 \leq \epsilon_c < \epsilon_{c0}$ ;

(ii) if  $\xi^*$  is an isolated local minimizer of the problem in (23) for given  $\rho > 0$  and  $\epsilon_c > 0$ , then there exists  $\epsilon_2 > 0$  such that

$$\|\xi^* - \xi_d\|_{L_2} \leq \|\xi - \xi_d\|_{L_2} + \epsilon_2$$

for all trajectories  $\xi \in \mathcal{T}$  in a neighborhood of  $\xi^*$ ;

(iii) for  $\xi^*$  as in (ii), then there exists  $\epsilon_3 > 0$  such that

$$\|p(x^*(\cdot)) - \mathbf{y}_d(\cdot)\|_{L_2} \leq \|p(x(\cdot)) - \mathbf{y}_d(\cdot)\|_{L_2} + \epsilon_3$$

for all trajectories  $\xi = (x(\cdot), u(\cdot)) \in \mathcal{T}$  in a neighborhood of  $\xi^* \in \mathcal{T}$ .

*Proof:* Statement (i) is just a straightforward corollary of Theorem 6.4. To prove statement (ii), we observe that from (i) there exists  $\delta > 0$  such that

$$\|\xi^* - \xi_d\|_{L_2} + \epsilon_c b_\rho(\xi^*) \leq \|\xi - \xi_d\|_{L_2} + \epsilon_c b_\rho(\xi)$$

for all  $\xi \in B(\xi^*, \delta)$ , so that

$$\|\xi^* - \xi_d\|_{L_2} \leq \|\xi - \xi_d\|_{L_2} + \epsilon_c (b_\rho(\xi) - b_\rho(\xi^*)).$$

Exploiting the structure of  $b_{\delta_c, \rho}$  and using the linearity of the integral operator we can write

$$b_{\delta_c, \rho}(\xi) - b_{\delta_c, \rho}(\xi^*) = \int_0^T \sum_j \beta(-c_j(x(\tau), u(\tau))) - \beta(-c_j(x^*(\tau), u^*(\tau))) d\tau$$

Using the fact that  $\beta$  is a  $\mathcal{C}^2$  function and each  $c_j$  is  $\mathcal{C}^2$  in both arguments (so that they are all bounded on  $[0, T]$ ), there exists  $c_2 > 0$  such that

$$b_{\delta_c, \rho}(\xi) - b_{\delta_c, \rho}(\xi^*) \leq T \max_{\tau \in [0, T]} \sum_j \beta(-c_j(x(\tau), u(\tau))) - \beta(-c_j(x^*(\tau), u^*(\tau))) \leq T c_2.$$

The result follows by choosing  $\epsilon_2 = \epsilon_c T c_2$ .

To prove statement (ii) we assume, without loss of generality, that the state vector can be written as  $x = [x_1^T \ x_2^T]^T$ , where  $x_1 \in \mathbb{R}^p$  is the vector of performance outputs, that is  $p(x) = x_1$ , and  $x_2 \in \mathbb{R}^{n-p}$  the remaining portion of the state. We use the same partition for any (state-input) curve so that, given a desired curve  $\xi_d \in \tilde{X}$ , a weighed  $L_2$  distance of a curve  $\xi \in \tilde{X}$  from a lifted trajectory  $\xi_d \in \mathcal{T}$  satisfies

$$\begin{aligned} \|\xi - \xi_d\|_{L_2} &\leq \frac{1}{2} \int_0^T \|x_1(\tau) - x_{1d}(\tau)\|_{Q_1}^2 + \|x_2(\tau) - x_{2d}(\tau)\|_{Q_2}^2 + \|u(\tau) - u_d(\tau)\|_R^2 d\tau \\ &\quad + \frac{1}{2} \|x_1(T) - x_{1d}(T)\|_{P_1}^2 + \frac{1}{2} \|x_2(T) - x_{2d}(T)\|_{P_2}^2 + c_3 \end{aligned} \quad (24)$$

where  $Q_1, Q_2, R, P_1$  and  $P_2$  are positive definite matrices and  $c_3 > 0$  is a positive constant taking into account cross terms. Now, rearranging terms in (24), we have

$$\begin{aligned} \|\xi - \xi_d\|_{L_2} &\leq \frac{1}{2} \int_0^T \|x_1(\tau) - x_{1d}(\tau)\|_{Q_1}^2 d\tau + \frac{1}{2} \|x_1(T) - x_{1d}(T)\|_{P_1}^2 + \\ &\quad \frac{1}{2} \int_0^T \|x_2(\tau) - x_{2d}(\tau)\|_{Q_2}^2 + \frac{1}{2} \|x_2(T) - x_{2d}(T)\|_{P_2}^2 + \frac{1}{2} \int_0^T \|u(\tau) - u_d(\tau)\|_R^2 d\tau + c_3 \\ &= \|p(x(\cdot)) - \mathbf{y}_d(\cdot)\|_{L_2} + \|x_2(\cdot) - x_{2d}(\cdot)\|_{L_2} + \|u(\cdot) - u_d(\cdot)\|_{L_2} + c_3, \end{aligned}$$



where we have used the fact that  $\xi_d$  is a lifted trajectory (and thus  $x_{1d}(\cdot) := p(x_d(\cdot)) = \mathbf{y}_d(\cdot)$ ) and supposed that the weighted  $L_2$  norm for the input has no terminal penalty. Using similar arguments, the converse inequality can be obtained, i.e.,  $\|\xi - \xi_d\|_{L_2} \geq \|p(x(\cdot)) - \mathbf{y}_d(\cdot)\|_{L_2} + \|x_2(\cdot) - x_{2d}(\cdot)\|_{L_2} + \|u(\cdot) - u_d(\cdot)\|_{L_2} - c_4$ , for a suitable  $c_4 > 0$ . It is worth noting that, if the weight matrices  $Q$ ,  $R$  and  $P_f$  are block diagonal the above inequalities are equalities with  $c_3 = c_4 = 0$ .

From (ii), we have that there exist  $\xi^* \in \mathcal{T}$  and  $\epsilon_2 > 0$  such that  $\|\xi^* - \xi_d\|_{L_2} \leq \|\xi - \xi_d\|_{L_2} + \epsilon_2$  for all  $\xi \in \mathcal{T}$  in a neighborhood of  $\xi^*$ . Thus, we can write

$$\begin{aligned} \|p(x^*(\cdot)) - \mathbf{y}_d(\cdot)\|_{L_2} + \|x_2^*(\cdot) - x_{2d}(\cdot)\|_{L_2} + \|u^*(\cdot) - u_d(\cdot)\|_{L_2} \leq \\ \|p(x(\cdot)) - \mathbf{y}_d(\cdot)\|_{L_2} + \|x_2(\cdot) - x_{2d}(\cdot)\|_{L_2} + \|u(\cdot) - u_d(\cdot)\|_{L_2} + \epsilon_2 + c_3 + c_4, \end{aligned}$$

and,

$$\begin{aligned} \|p(x^*(\cdot)) - \mathbf{y}_d(\cdot)\|_{L_2} \leq \|p(x(\cdot)) - \mathbf{y}_d(\cdot)\|_{L_2} + \\ (\|x_2(\cdot) - x_{2d}(\cdot)\|_{L_2} - \|x_2^*(\cdot) - x_{2d}(\cdot)\|_{L_2} + \|u(\cdot) - u_d(\cdot)\|_{L_2} - \|u^*(\cdot) - u_d(\cdot)\|_{L_2} + \epsilon_2 + c_3 + c_4). \end{aligned}$$

Using the same arguments on boundedness of the state and input trajectories and boundedness of the weighted  $L_2$  norm on a neighborhood of  $\xi^*$  as in (ii), we have that there exists  $\epsilon_3 > 0$  such that  $\|p(x^*(\cdot)) - \mathbf{y}_d(\cdot)\|_{L_2} \leq \|p(x(\cdot)) - \mathbf{y}_d(\cdot)\|_{L_2} + \epsilon_3$ , thus concluding the proof.  $\blacksquare$

**Remark 6.7 (Analysis of the lift and constraint strategy for the PVTOL)** *The initialization part of the lift and constrain strategy for the PVTOL can be easily performed. Indeed, the  $LIFT_0$  procedure simply implements equations in (4). Then we proceed by analyzing each step. As for Step 1, we can use Theorem 4.6 to prove that there exists  $\epsilon_{P0} > 0$  such that for any  $\epsilon_P < \epsilon_{P0}$  an unconstrained lifted trajectory for the coupled PVTOL exists and depends continuously on the coupling parameter. Thus, we know that for “small” positive values of the coupling parameter the continuation procedure will be successful, thus providing an unconstrained desired trajectory for the following continuation steps. Using Theorem 6.6 (i), we have that for feasibility regions that are not too tight Step 2 and Step 3 will be successful and, thus, a feasible trajectory that locally solves the practical feasible lifting task can be found.*

## 7 Numerical computations on the PVTOL

In this section we present numerical computations showing the effectiveness of the proposed strategy on the PVTOL. We proceed defining the feasibility region (equivalently the point-wise constraints that the system trajectories must satisfy) and the desired maneuver. Regarding the feasibility region, we consider the case of constraining the input only, i.e.  $u_1$  and  $u_2$  are bounded with, in particular,  $u_1$  strictly positive. In order to have a compact feasibility region we just assume that the states must belong to a sufficiently large compact and simply connected set  $\Omega \subset \mathbb{R}^6$  such that the state portion of the trajectory is for sure feasible. The feasibility set is thus defined as

$$\overline{\mathcal{XU}} = \{(x, u) \in \Omega \times \mathbb{R}^2 \mid 0 < u_{1\min} \leq u_1 \leq u_{1\max}, u_{2\min} \leq u_2 \leq u_{2\max} \text{ for given } u_{1\min}, u_{1\max}, u_{2\min} \text{ and } u_{2\max}\}.$$

Then, we parametrize the feasibility region with the scaling parameter  $\rho$  and define the inequalities determining the barrier functional. We pose the inequalities in terms of the square distance of  $u_1$  and  $u_2$  from the boundary values in order to have a smooth barrier functional. The two inequalities are as follows

$$\begin{aligned} \left[ u_1 - \frac{(u_{1\max} + u_{1\min})}{2} \right]^2 &\leq \left[ (\rho + (1 - \rho)k_1) \frac{(u_{1\max} - u_{1\min})}{2} \right]^2 \\ \left[ u_2 - \frac{(u_{2\max} + u_{2\min})}{2} \right]^2 &\leq \left[ (\rho + (1 - \rho)k_2) \frac{(u_{2\max} - u_{2\min})}{2} \right]^2 \end{aligned}$$

where we set  $u_{1\min} = 0.5g$  ( $g$  being the gravity constant),  $u_{1\max} = 1.5g \text{ m/s}^2$ ,  $u_{2\min} = -80 \text{ deg/s}^2$ ,  $u_{2\max} = 80 \text{ deg/s}^2$ , while  $k_1$  and  $k_2$  are two scaling factors that guarantee feasibility for  $\rho = 0$ .

Regarding the desired maneuver, we aim at performing a barrel roll with a constant velocity profile. Specifically, we choose the desired outputs,  $y_d(\cdot)$  and  $z_d(\cdot)$ , so that the desired path is the one depicted in Figure 3a and the velocity is  $v_d = 10m/s$ .

We are now ready to present the results of the main steps of the lift and constrain strategy for the described feasibility region and desired maneuver. A lifted trajectory for the decoupled PVTOL ( $\epsilon_P = 0$ ) is computed according to Equations (4). Recall that this trajectory is a quasi-static trajectory for any coupled PVTOL. Then, using the dynamic embedding technique described in Section 5, we compute a lifted trajectory for the coupled PVTOL with nominal parameter  $\epsilon_P = 1$ . We solve the optimal control problem by using the projection operator Newton method. The quasi-static versus lifted path is depicted in Figure 3 together with the velocity and roll trajectories. The

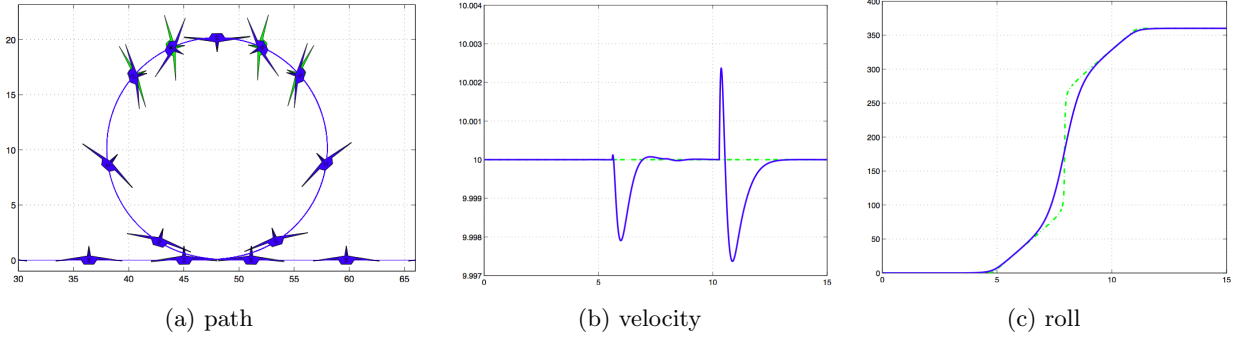


Fig. 3. Quasi-static (decoupled PVTOL) vs lifted (coupled PVTOL) path, velocity and roll trajectories for the unconstrained PVTOL ( $\epsilon_P = 1$ ). Specifically: the dashed green lines are the quasi-static curves, while the solid blue are the lifted trajectories.

decoupled versus coupled roll-rate and input trajectories are depicted in Figure 4. As appears from the picture, the

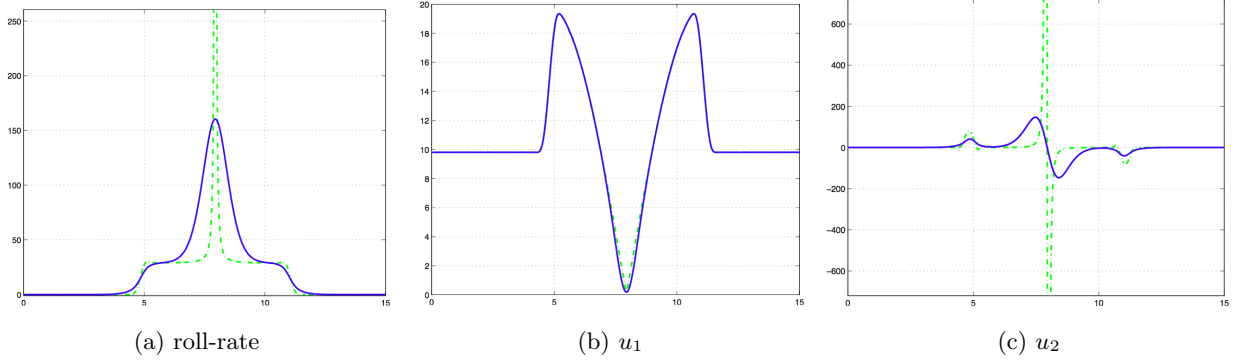


Fig. 4. Quasi-static (decoupled PVTOL) vs lifted (coupled PVTOL) roll rate and input trajectories for the unconstrained PVTOL ( $\epsilon_P = 1$ ). Specifically: the dashed green lines are the quasi-static curves, while the solid blue are the lifted trajectories.

desired and lifted paths and velocities are indistinguishable (the maximum error is of order  $10^{-3}$  consistent with the required absolute tolerance). This is consistent with the result in Theorem 4.6 stating that the lifting task can be solved exactly for some positive values of  $\epsilon_P$ . As expected the roll and roll rate trajectories and the input trajectories are significantly different from the quasi-static ones. In particular, the optimal roll and roll rate trajectories display a degree of anticipation and are smoother than the quasi-static. This is due to the filtering action of the dynamics. This filtering effect can be seen also in the snapshots of the PVTOL animation in Figure 3a. It is worth noting that neither the desired nor the lifted trajectory satisfy the constraints and, thus, are both infeasible.

Now, we are ready to show the results of the “constrain” part of the strategy. As regards the  $L_2$  weights, we choose diagonal  $Q$  and  $R$  matrices (for simplicity) and penalize the outputs (external position states)  $10^4$  times the other states and the inputs. We initialize the strategy by setting  $\epsilon_c = 10$ . We choose a relatively high value for  $\epsilon_c$  so that for each given value of  $\rho$  the trajectory that we find is sufficiently far from the boundary. This has two advantages. First, when we increase  $\rho$ , thus shrinking the feasibility region, the constraints are only slightly violated if the step-size on  $\rho$  is not too large. Second, once  $\rho = 1$  has been reached, we can converge to a tighter approximation ( $\epsilon_c \rightarrow 0$ ) in an

interior point fashion. The parameter  $\rho$  is varied with a step-size of 0.2. For each value of  $\rho$  the minimization takes few (less than 5) Newton iterations (with an absolute tolerance on the descent direction set to  $10^{-6}$ ). Once reached the value  $\rho = 1$ ,  $\epsilon_c$  is decreased down to  $\epsilon_c = 0.1$ .

The desired versus feasible path, velocity and roll trajectories are depicted in Figure 5 (for  $\rho = 1$  and  $\epsilon_c = 0.1$ ). Snapshots of the PVTOL animation are shown Figure 5a as for the unconstrained case. For the velocity and roll angle we also plot intermediate non-optimal trajectories obtained during the continuation procedure. In particular we plot the trajectories obtained for  $\rho = 0.6$  and  $\rho = 1$  with  $\epsilon_c = 10$ . It is interesting to notice that even in presence

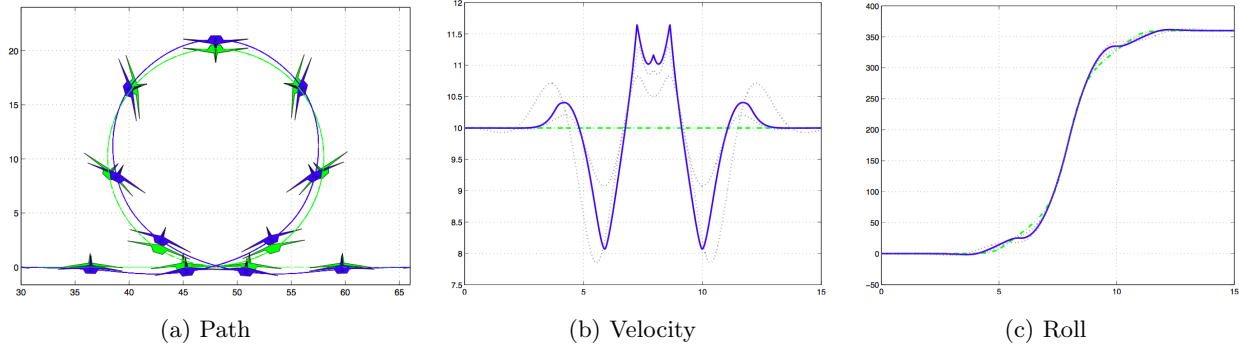


Fig. 5. Desired vs feasible path, velocity and roll angle for the coupled PVTOL ( $\epsilon_P = 1$ ). Specifically: the dashed green lines are the desired infeasible curves, the solid blue lines are the feasible optimal trajectories ( $\rho = 1$  and  $\epsilon_c = 0.1$ ), and (for velocity and roll angle) the thinner dotted grey lines are intermediate trajectories obtained for  $\rho = 0.6$  and  $\rho = 1$  with  $\epsilon_c = 10$  respectively.

of tight constraints on the two inputs the feasible trajectory output (path and velocity) is reasonably close to the desired one. The maximum error on  $y(\cdot)$  and  $z(\cdot)$  is less than 1m and the maximum error on the velocity is less than 2m/s. Also, it is worth noting that the roll trajectory, Figure 5c, stays bounded and relatively close to the desired one even if the weight in the cost function is much lower than the one on the positions.

In Figure 6 we show the feasible versus desired roll-rate and inputs for the same values of  $\rho$  and  $\epsilon_c$ . The controls have a bang-bang like behavior. In particular they tend to assume the boundary value in a larger interval than the one on which the constraints are violated in order to compensate the missing control effort in the infeasible time windows. This non-causal behavior shows that, in order to obtain performances that are comparable with the unconstrained case the optimization needs to work in a non-causal fashion.

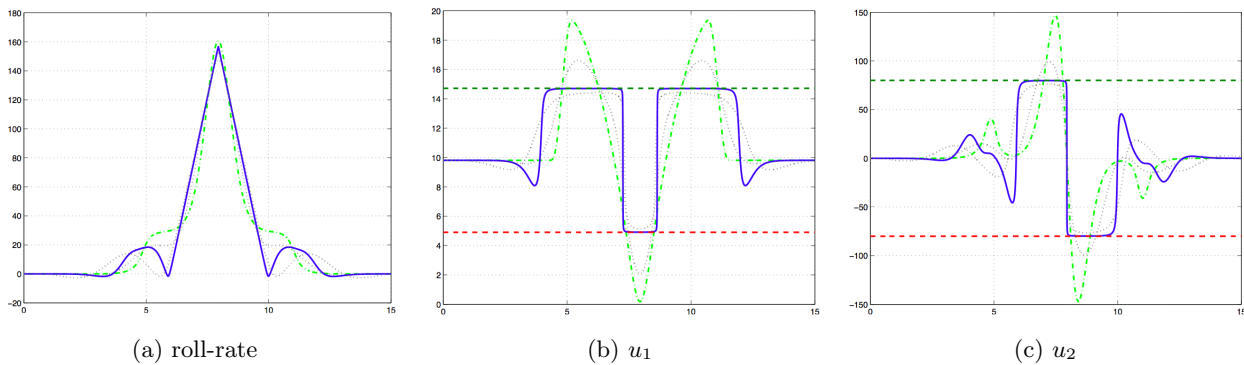


Fig. 6. Desired vs feasible roll-rate,  $u_1$  and  $u_2$  for the coupled PVTOL ( $\epsilon_P = 1$ ). Specifically: the dashed green lines are the desired infeasible curves, the solid blue lines are the optimal trajectories ( $\rho = 1$  and  $\epsilon_c = 0.1$ ), and the thinner dotted grey lines are intermediate trajectories (obtained for  $\rho = 0.6$  and  $\rho = 1$  with  $\epsilon_c = 10$  respectively).

The results obtained in the above computations show that the inputs tend to be discontinuous when  $\epsilon_c \rightarrow 0$  thus suggesting that the constrained minimizer is, in fact, discontinuous. In order to have a smoother input we could vary the parameters of the strategy. We could, e.g., increase the parameter  $\epsilon_c$  thus obtaining a smoother trajectory (as the intermediate feasible trajectory shown in Figure 6 in dotted grey line) or increase the  $L_2$  input weights (the

coefficients of the matrix  $R$ ). Both the two procedures increase the error on the desired output. Next, we show a different procedure to obtain the same input regularization without losing too much in terms of output error. This procedure allows us to show that the proposed strategy can easily deal with both state and input constraints without any increase in the complexity of the strategy. We proceed by applying a dynamic extension to the system, [18]. In the extended system the actual inputs are two additional states, while their derivatives are the new inputs.

$$\begin{aligned}\dot{x} &= f(x, w) \\ \dot{w} &= v,\end{aligned}$$

where  $x = [y \ z \ \varphi \ \dot{y} \ \dot{z} \ \dot{\varphi}]$  and  $w = [u_1 \ u_2]$  are the states of the extended system and  $v = [\dot{u}_1 \ \dot{u}_2]$  is the input.

The results are shown in Figure 7. We compare the feasible path and original inputs ( $u_1$  and  $u_2$ ) obtained with and without dynamic extension. In particular, for the extended system both the original inputs (additional states) and the original input derivatives (new inputs) are constrained.

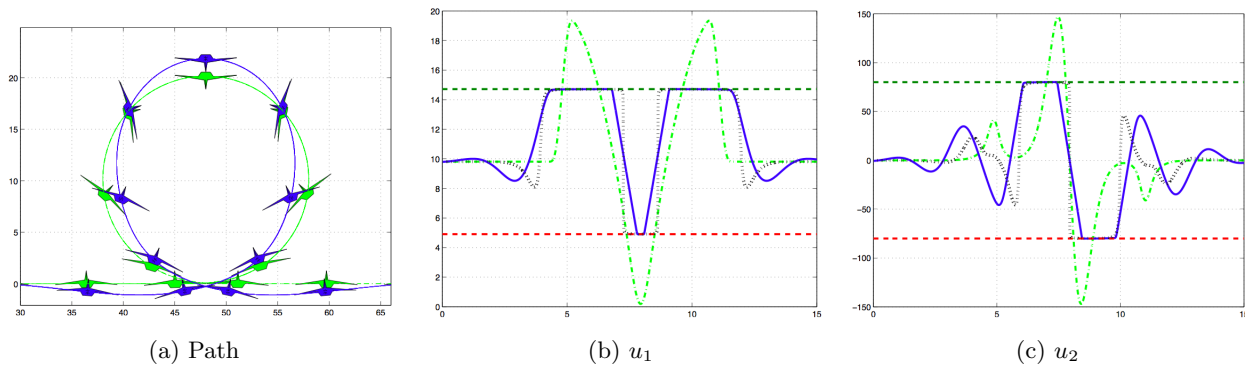


Fig. 7. Desired vs feasible path and inputs for the coupled PVTOL ( $\epsilon_P = 1$ ) with and without bounds on the input derivatives. Specifically: the dashed green lines are the desired curves, the solid blue lines are the optimal trajectories for the system with dynamic extension (bounds on both inputs and input derivatives) and the dotted grey lines are the optimal trajectories for the system without dynamic extension (bounds on the inputs only).

## 8 Conclusions

In this paper we have studied a constrained trajectory lifting problem for nonlinear control systems. Given a desired output curve for a nonlinear *maneuvering* system, we compute a full (state-input) trajectory of the system such that: (i) the output portion is close to the desired one, and (ii) a set of point-wise state-input constraints are satisfied. We have proposed a nonlinear optimal control strategy based on a novel projection operator based Newton method for point-wise constrained control systems [10,12] combined with dynamic embedding, constraints relaxation and continuation with respect to parameters. Under suitable values of the system and constraints parameters we have proven that a feasible trajectory exists and can be computed by means of the proposed strategy. Finally, we have completely characterized the strategy for the PVTOL aircraft and provided numerical computations showing the effectiveness of the strategy for an aggressive desired barrel roll maneuver in presence of relatively tight constraints.

## References

- [1] S. A. Al-Hiddabi and N. H. McClamroch. Tracking and maneuver regulation control for nonlinear nonminimum phase systems: application to flight control. *IEEE Transactions on Control Systems Technology*, 10(6), 2002.
- [2] S. Boyd and L. Vandenberghe. *Convex Optimization*. Cambridge University Press, 2004.
- [3] A. Isidori C. I. Byrnes. Output regulation for nonlinear systems: an overview. *International Journal of Robust and Nonlinear Control*, 10:323–337, 2000.
- [4] L. Consolini, M. Maggiore, C. Nielsen, and M. Tosques. Path following for the PVTOL aircraft. *Automatica*, 46:1284–1296, 2010.
- [5] L. Consolini and M. Tosques. On the VTOL exact tracking with bounded internal dynamics via a poincaré map approach. *IEEE Transactions on Automatic Control*, 52:1757–1762, 2007.
- [6] S. Devasia. Approximated stable inversion for nonlinear systems with nonhyperbolic internal dynamics. *IEEE Transactions on Automatic Control*, 44(7):1419–1425, July 1999.

- [7] S. Devasia, D. Chen, and B. Paden. Nonlinear inversion-based output tracking. *IEEE Transactions on Automatic Control*, 41(7):930–942, July 1996.
- [8] S. Devasia and B. Paden. Stable inversion for nonlinear nonminimum-phase time-varying systems. *IEEE Transactions on Automatic Control*, 43(2):283–288, February 1998.
- [9] N. H. Getz and J. E. Marsden. Control for an autonomous bicycle. In *IEEE Int. Conf. on Robotics and Automation*, volume 2, pages 1397–1402, May 1995.
- [10] J. Hauser. A projection operator approach to the optimization of trajectory functionals. In *IFAC World Congress*, Barcelona, 2002.
- [11] J. Hauser and D. G. Meyer. The trajectory manifold of a nonlinear control system. In *IEEE Conf. on Decision and Control*, volume 1, pages 1034–1039, December 1998.
- [12] J. Hauser and A. Saccon. A barrier function method for the optimization of trajectory functionals with constraints. In *IEEE Conf. on Decision and Control*, pages 864–869, San Diego, Dec 2006.
- [13] J. Hauser, A. Saccon, and R. Frezza. Aggressive motorcycle trajectories. In *IFAC Symposium on Nonlinear Control Systems*, Stuttgart, 2004.
- [14] J. Hauser, A. Saccon, and R. Frezza. On the driven inverted pendulum. In *IEEE Conf. on Decision and Control and European Control Conference*, pages 6176–6180, Dec. 2005.
- [15] J. Hauser, S. Sastry, and G. Meyer. Nonlinear control design for slightly nonminimum phase systems: Application to V/STOL aircraft. *Automatica*, 28(4):665–679, 1992.
- [16] J. Huang. *Nonlinear output regulation. Theory and applications*. SIAM, Philadelphia, 2004.
- [17] L.R. Hunt and G. Meyer. Stable inversion for nonlinear-systems. *Automatica*, 33(8):1549–1554, 1997.
- [18] A. Isidori. *Nonlinear Control Systems*. Communications and Control Engineering Series. Springer, 3 edition, 1995.
- [19] A. Isidori and C.I. Byrnes. Output regulation of nonlinear systems. *IEEE Transactions on Automatic Control*, 35(2):131–140, February 1990.
- [20] A. Isidori, L. Marconi, and A. Serrani. *Robust Autonomous Guidance. An Internal Model Approach*. Advances in Industrial Control. Springer, 2003.
- [21] L. Marconi, A. Isidori, and A. Serrani. Autonomous vertical landing on an oscillating platform: an internal model based approach. *Automatica*, 38:21–32, 2002.
- [22] H. Maurer and H. J. Pesch. Solution differentiability for nonlinear parametric control problems. *SIAM Journal on Control and Optimization*, 32(6):1542–1554, 1994.
- [23] H. Maurer and H. J. Pesch. Solution differentiability for parametric nonlinear control problems with control-state constraints. *Journal of Optimization Theory and Applications*, 86(2):285–309, 1995.
- [24] R. Naldi and L. Marconi. Optimal transition maneuvers for a class of V/STOL aircraft. *Automatica*, 47, 2011.
- [25] G. Notarstefano, J. Hauser, and R. Frezza. Computing feasible trajectories for control-constrained systems: the PVTOL aircraft. In *IFAC Symposium on Nonlinear Control Systems*, Pretoria, SA, August 2007.
- [26] G. Notarstefano, J. Hauser, and R. Frezza. Trajectory manifold exploration for the PVTOL aircraft. In *IEEE Conf. on Decision and Control and European Control Conference*, pages 5848–5853, Seville, December 2005.
- [27] A. Pavlov, N. Van de Wouw, and H. Nijmeijer. Global nonlinear output regulation: Convergence-based controller design. *Automatica*, 43:456–463, 2007.
- [28] A. Pavlov and K. Y. Pettersen. A new perspective on stable inversion of non-minimum phase nonlinear systems. *Modeling, Identification and Control*, 29(1):29–35, 2008.
- [29] P. Martin, S. Devasia, and B. Paden. A different look at output tracking: control of a VTOL aircraft. *Automatica*, 32(1):101–107, 1996.
- [30] M. W. Spong and D.J. Block. The pendubot: a mechatronic system for control research and education. In *IEEE Conf. on Decision and Control*, pages 555–556, December 1995.
- [31] Eberhard Zeidler. *Applied Functional Analysis: Main Principles and their applications*. Springer-Verlag, New York, 1995.

## A The *Projection Operator* approach for the optimization of trajectory functionals

In this section we recall the main mathematical tools that we use to develop the feasible trajectory exploration strategy and to prove its correctness.

### A.1 Trajectory tracking projection operator

The trajectory tracking projection operator, [11], provides a numerically robust representation of nonlinear system trajectories and is at the basis of the novel descent methods for nonlinear optimization of trajectory functionals, [10], used in the paper. Let us consider the nonlinear control system  $\dot{x}(t) = f(x(t), u(t))$ ,  $x(0) = x_0$ , where  $f(x, u)$  is a  $C^2$  map in  $x \in \mathbb{R}^n$  and  $u \in \mathbb{R}^m$ . We recall that a *bounded curve*  $\eta = (\bar{x}(\cdot), \bar{u}(\cdot))$  is a (state-input) *trajectory*

of the system if  $\dot{\bar{x}}(t) = f(\bar{x}(t), \bar{u}(t))$ ,  $\bar{x}(0) = x_0$ , for all  $t \in [0, T]$ ,  $0 < T \leq +\infty$ . Suppose that  $\xi(t) = (\alpha(t), \mu(t))$ ,  $t \in [0, T]$ , is a bounded curve (e.g., an approximate trajectory of the system) and let  $\eta(t) = (x(t), u(t))$ ,  $t \in [0, T]$ , be the trajectory determined by the nonlinear feedback system

$$\begin{aligned}\dot{x}(t) &= f(x(t), u(t)), & x(0) &= x_0, \\ u(t) &= \mu(t) + K(t)(\alpha(t) - x(t))\end{aligned}$$

Under certain conditions on  $f$  and  $K$ , this feedback system defines a continuous, nonlinear *projection operator*

$$\mathcal{P} := (\alpha, \mu) \mapsto \eta = (x, u).$$

That is, independent of  $K$ , if  $\xi$  is a trajectory,  $\xi \in \mathcal{T}$ , then  $\xi$  is a fixed point of  $\mathcal{P}$ ,  $\xi = \mathcal{P}(\xi)$ . If  $K$  is bounded (and, if  $\xi$  is a trajectory of infinite extent, such that the above feedback exponentially stabilizes  $\xi_0$ ), then  $\mathcal{P}$  is well defined on an  $L_\infty$  neighborhood of  $\xi_0$  and is  $\mathcal{C}^r$  (with respect to the  $L_\infty$  norm) on its domain (including an open neighborhood of  $\xi_0$ ) whenever  $f$  is [10]. The first derivative of the projection operator,  $\zeta \mapsto D\mathcal{P}(\xi) \cdot \zeta$ , is the (continuous) linear projection operator given by the standard linearization

$$\begin{aligned}\dot{z}(t) &= A(\eta(t))z(t) + B(\eta(t))v(t), & z(0) &= 0, \\ v(t) &= \nu(t) + K(t)[\beta(t) - z(t)].\end{aligned}$$

where  $D\mathcal{P}(\xi) \cdot \zeta = (z(\cdot), v(\cdot))$ , with  $\zeta = (\beta(\cdot), \nu(\cdot))$ , and  $A(\eta(t)) = f_x(x(t), u(t))$  and  $B(\eta(t)) = f_u(x(t), u(t))$ . The tangent space  $T_\xi \mathcal{T}$  at a given trajectory  $\xi \in \mathcal{T}$  is, thus, the set of curves  $\zeta$  satisfying  $\zeta = D\mathcal{P}(\xi) \cdot \zeta$ .

The projection operator  $\mathcal{P}$  provides a convenient parametrization of the trajectories in the neighborhood of a given trajectory [11]. Indeed, the tangent space  $T_\xi \mathcal{T}$  can be used to parameterize all nearby trajectories.

**Theorem A.1 (Trajectory manifold representation theorem [11])** *Given  $\xi \in \mathcal{T}$ , there is an  $\epsilon > 0$  such that, for each  $\eta \in \mathcal{T}$  with  $\|\eta - \xi\|_{L_\infty} < \epsilon$  there is a unique  $\zeta \in T_\xi \mathcal{T}$  such that  $\eta = \mathcal{P}(\xi + \zeta)$ . This provides a  $\mathcal{C}^r$  atlas of charts, indexed by trajectories  $\xi \in \mathcal{T}$ , so that  $\mathcal{T}$  is a  $\mathcal{C}^r$  Banach manifold.*

## A.2 Projection operator based Newton method

Consider the unconstrained optimal control problem

$$\begin{aligned}\text{minimize } & \int_0^T l(\tau, x(\tau), u(\tau)) d\tau + m(x(T)) \\ \text{subj. to } & \dot{x}(t) = f(x(t), u(t)), \quad x(0) = x_0.\end{aligned}\tag{A.1}$$

where  $l(t, x, u)$  is  $\mathcal{C}^2$  in  $x$  and  $u$ , convex in  $u$ , and  $\mathcal{C}^1$  in  $t$ , and  $m(x)$  is  $\mathcal{C}^2$  in  $x$ . This problem is equivalent to the constrained optimization problems

$$\min_{\xi \in \mathcal{T}} h(\xi) = \min_{\xi = \mathcal{P}(\xi)} h(\xi).$$

where  $h(\xi) := \int_0^T l(\tau, x(\tau), u(\tau)) d\tau + m(x(T))$  and the constraint set, the trajectory space  $\mathcal{T}$ , is a Banach submanifold of  $\tilde{X} = (x_0, 0) + X_\infty$ . Next lemma is the basis for the Projection Operator Newton descent method that we use in our strategy. This result is also useful to prove the existence of a feasible lifted trajectory.

**Lemma A.2 (Unconstrained minimization through projection [10])** *Let  $g(\xi) := h(\mathcal{P}(\xi))$ , for  $\xi \in \mathcal{U} \subset \tilde{X}$  with  $\mathcal{P}(\mathcal{U}) \subset \mathcal{U} \subset \text{dom } \mathcal{P}$ . Then, the optimization problems*

$$\min_{\xi \in \mathcal{T}} h(\xi) \quad \text{and} \quad \min_{\xi \in \mathcal{U}} g(\xi)$$

*are equivalent in the following sense. If  $\xi^* \in \mathcal{T} \cap \mathcal{U}$  is a constrained local minimum of  $h$ , then it is an unconstrained local minimum of  $g$ . If  $\xi^+ \in \mathcal{U}$  is an unconstrained local minimum of  $g$  in  $\mathcal{U}$ , then  $\xi^* = \mathcal{P}(\xi^+)$  is a constrained local minimum of  $h$  on  $\mathcal{T}$ .*

The projection operator based Newton method, [10], is the following.

---

**Algorithm** (projection operator Newton method)

Given initial trajectory  $\xi_0 \in \mathcal{T}$

**For**  $i = 0, 1, 2, \dots$

    design  $K$  defining  $\mathcal{P}$  about  $\xi_i$

    search direction:

$$\zeta_i = \arg \min_{\zeta \in T_{\xi_i} \mathcal{T}} Dg(\xi_i) \cdot \zeta + \frac{1}{2} D^2 g(\xi_i)(\zeta, \zeta)$$

    step size:  $\gamma_i = \arg \min_{\gamma \in (0,1]} g(\xi + \gamma \zeta_i)$ ;

    project:  $\xi_{i+1} = \mathcal{P}(\xi_i + \gamma_i \zeta_i)$ .

**end**

---

It is worth noting that the two main steps of designing the  $K$  and searching for the descent direction involve the solution of suitable (well known) LQ optimal control problems.

### A.3 Barrier functional approach for constrained optimal control

Next, we present an interior point method, introduced in [12], for the optimization of trajectory functionals in presence of point-wise state and input constraints. The objective is to solve over the class of bounded inputs the optimization problem (A.1) subject to the point-wise inequality constraints

$$c_j(t, x(t), u(t)) \leq 0, \quad j \in \{1, \dots, k\}, \quad \text{for almost all } t \in [0, T],$$

where  $c_j(t, x, u)$  is  $\mathcal{C}^2$  in  $(x, u)$  and  $\mathcal{C}^1$  in  $t$ . The main idea proposed in [12] is to approximate the solution of the constrained problem by solving an unconstrained optimal control problem through a suitable translation of the well known barrier function method used in finite dimension convex optimization [2]. The direct translation to infinite dimension would be

$$\begin{aligned} & \text{minimize} \quad \int_0^T l(\tau, x(\tau), u(\tau)) - \epsilon_c \sum_j \log(-c_j(t, x(\tau), u(\tau))) d\tau + m(x(T)) \\ & \text{subj. to} \quad \dot{x}(t) = f(x(t), u(t)), \quad x(0) = x_0 \end{aligned} \tag{A.2}$$

A key difficulty of the problem in (A.2) is that the cost functional can not be evaluated at infeasible curves. The problem is resolved by introducing the approximate barrier function  $\beta_{\delta_c}(\cdot)$ ,  $0 < \delta_c \leq 1$ , defined as

$$\beta_{\delta_c}(z) = \begin{cases} -\log z & z > \delta_c \\ \frac{k-1}{k} \left[ \left( \frac{z-k\delta_c}{(k-1)\delta_c} \right)^k - 1 \right] - \log \delta_c & z \leq \delta_c. \end{cases}$$

The associated barrier functional is

$$b_{\delta_c}(\xi) = \int_0^T \sum_j \beta_{\delta_c}(-c_j(\tau, \alpha(\tau), \mu(\tau))), \tag{A.3}$$

which is well defined for any curve  $\xi \in \tilde{X}$ , so that we get the optimal control problem relaxation

$$\min_{\xi \in \mathcal{T}} h(\xi) + \epsilon_c b_{\delta_c}(\xi).$$

**Remark A.3 (Projection operator Newton method to solve the relaxed problem)** *The projection operator Newton method can be used to optimize the functional  $g_{\epsilon_c, \delta_c}(\xi) = h(\mathcal{P}(\xi)) + \epsilon_c b_{\delta_c}(\mathcal{P}(\xi))$  as part of a continuation*

method on the parameters  $\epsilon_c$  and  $\delta_c$ . The technique is to start with a large  $\epsilon_c$  and  $\delta_c$ , solve the problem  $\min g_{\epsilon_c, \delta_c}(\xi)$  using the Newton method starting from the current trajectory and then reduce  $\epsilon_c$  and  $\delta_c$ . It is worth noting that for a fixed  $\epsilon_c$  it is possible to iterate on  $\delta_c$  up to a value for which the solution is the same as the pure barrier functional. For this reason in the paper we neglect the dependence of  $g_{\epsilon_c, \delta_c}(\xi)$  on  $\delta_c$  (thus writing  $g_{\epsilon_c}(\xi)$ ).